Funded by the
Erasmus+ Programme
of the European Union

Vibration energy harvesting systems

Francesco Cottone

NiPS laboratory, Department of Physics and Geology,
Università di Perugia, Italy

ERASMUS + IESRES
INNOVATIVE EUROPEAN STUDIES on RENEWABLE ENERGY SYSTEMS
Teaching Activity
27th June– 1st July 2016 - Pitesti, Romania

Outline

- Energy harvesting applications and principles
- Fundamentals of vibration energy harvesters
- Beyond linear systems
- Microscale energy harvesters
- Final considerations

Energy harvesting applications

Structural Monitoring

02/07/2014 - Belo Horizonte (Brazil)
(birdge collapse at FIAT factory)

Environmental Monitoring

Transportation

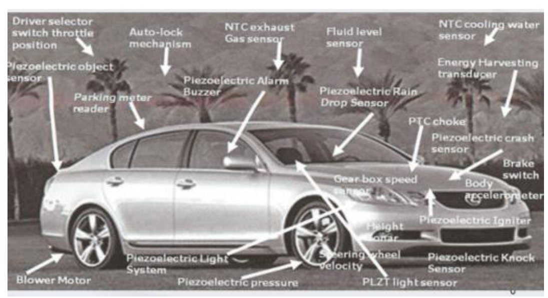

Wearable sensing for health applications

Emergency medical response
Monitoring, pacemaker, defibrillators

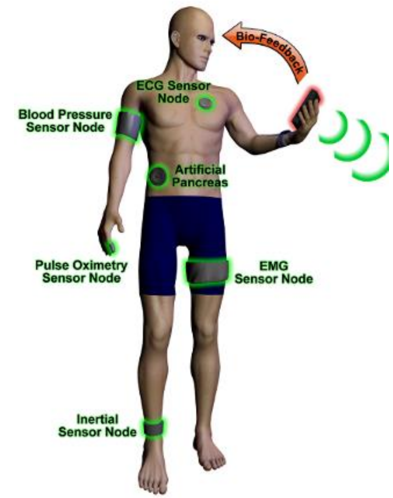

Military applications

Wireless Sensor Networks

Energy Harvesting could enable 90% of WSNs applications (IdTechex)

Power sources available from the ambient

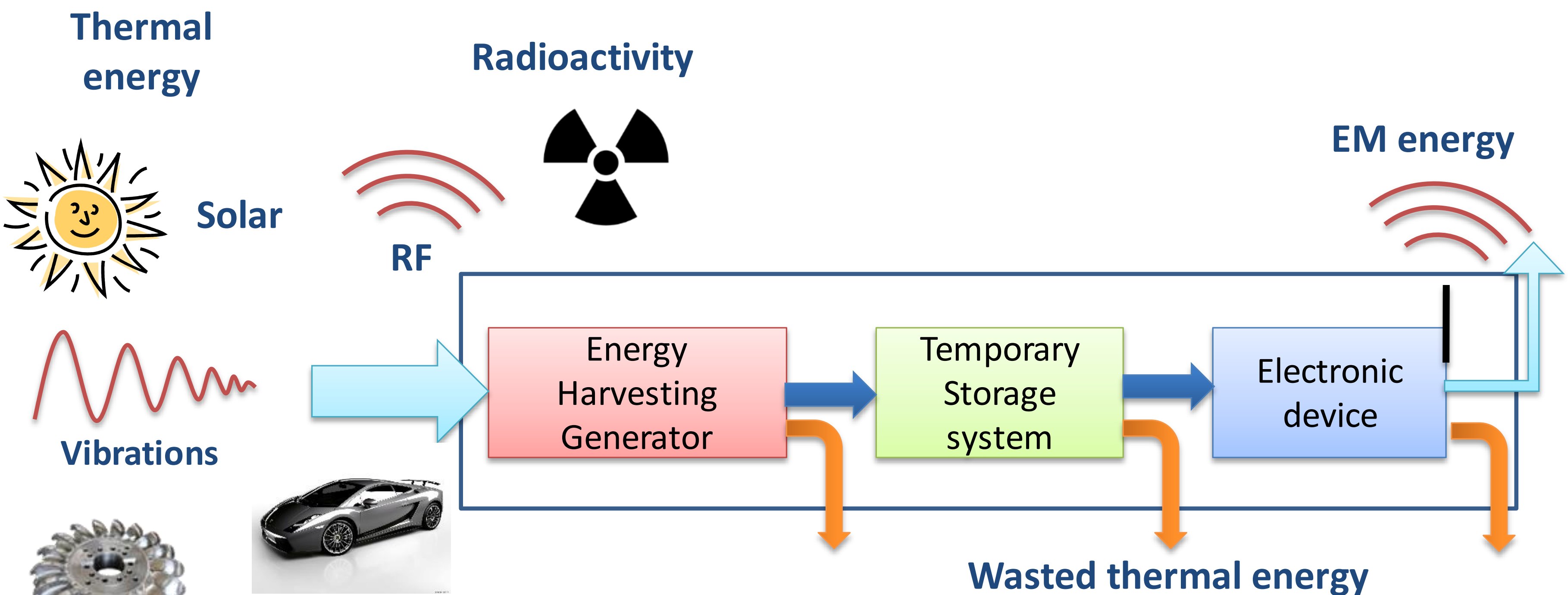

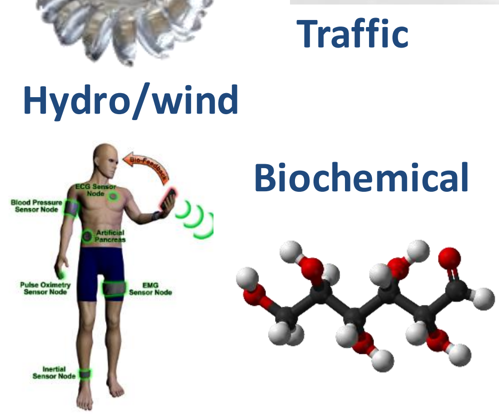

- Piezoelectric
- Electrodynamics
- Photovoltaic
- Hydro Turbine

- Ultra capacitors
- Rechargeable Batteries

- Wireless Sensor Node

Human-made energy harvesters

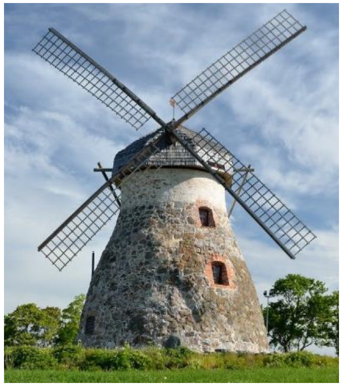

Wind mill (Origin: Persia, 3000 years BC)

Sailing ship (XVI-XVII century)

Crystal radio - 1906

SELF-powered by Radio Frequencies !!!

First automatic wristwatch, Harwood, c. 1929 (Deutsches Uhrenmuseum, Inv. 47-3543)

First automatic watch. [Abraham-Louis Perrelet](), Le Locle. 1776

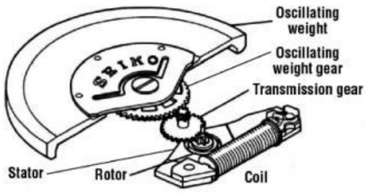

Self-charging Seiko wristwatch

Vibration powered wireless sensor

Power density objective for EH:

> 100 μW/cm³

Temporary storage and conditioning electrinics:

- *Ultra capacitors*
- *Rechargeable Batteries*

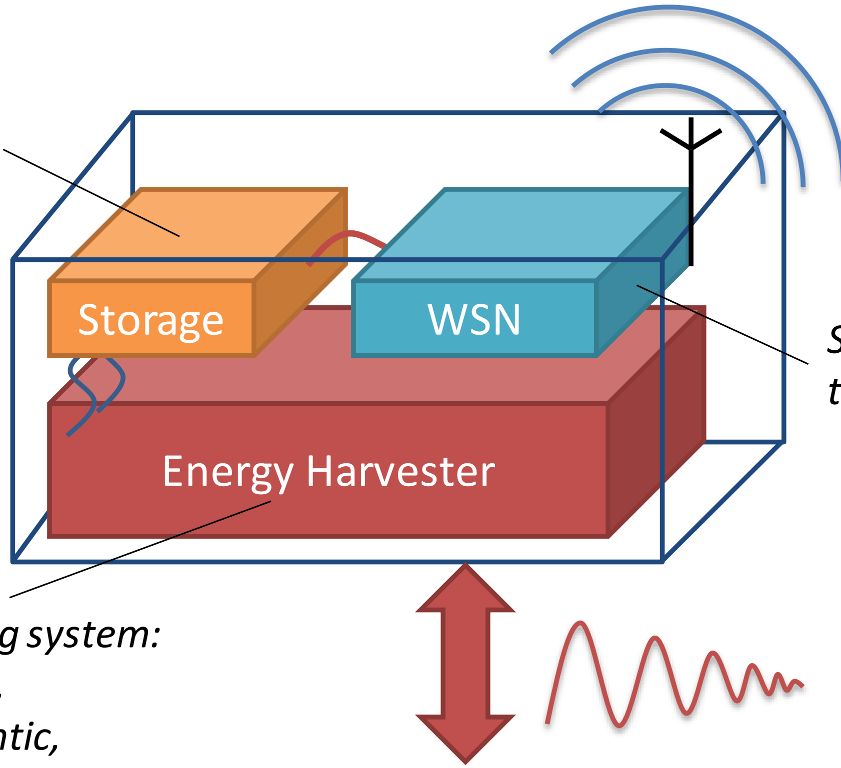

Sensor node and transceiver

Energy harvesting system:

- *piezoelectric,*
- *electromagentic,*
- *electrostatic,*
- *magnetostrictive*

Mechanical vibrations

Mobile devices: power needs

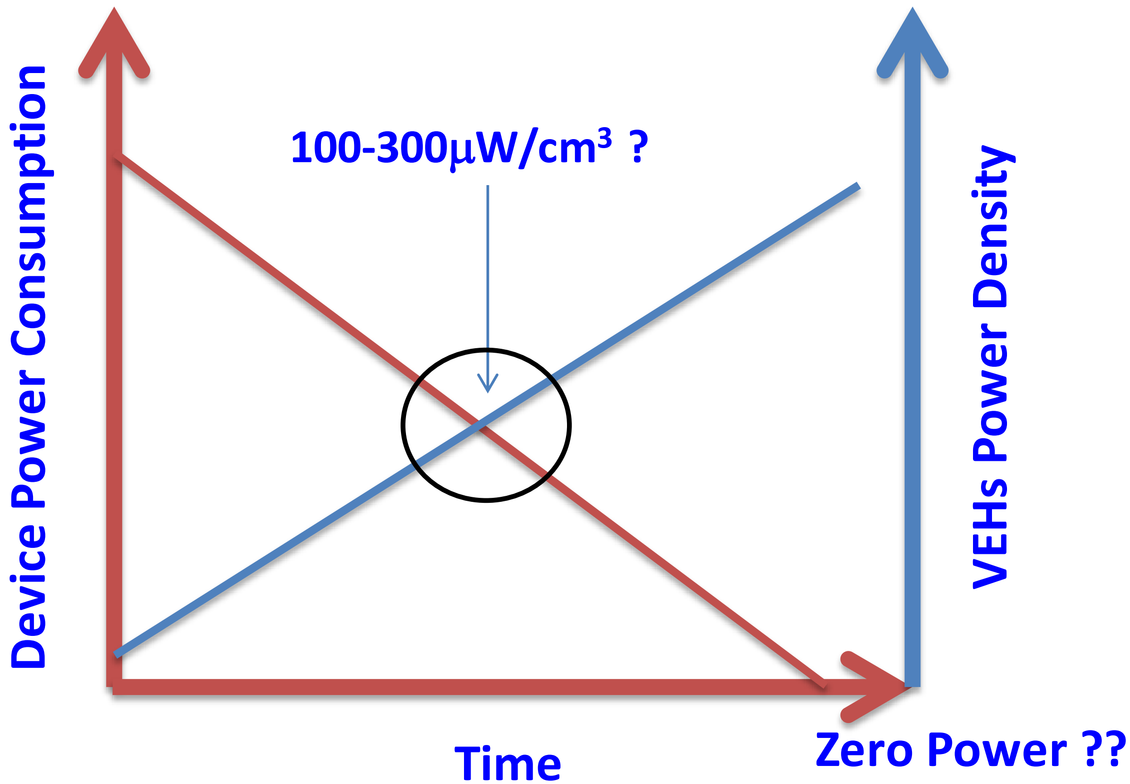

Vibration energy harvesting

Electromagnetic

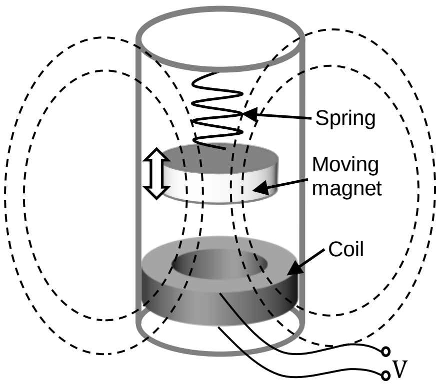

Electrostatic/Capacitive

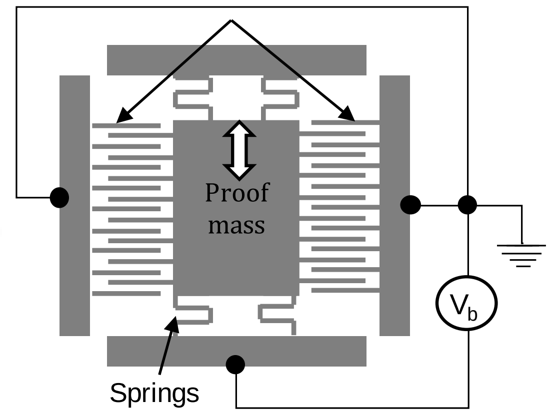

Vibration Harvesting Generator

Magnetostrictive

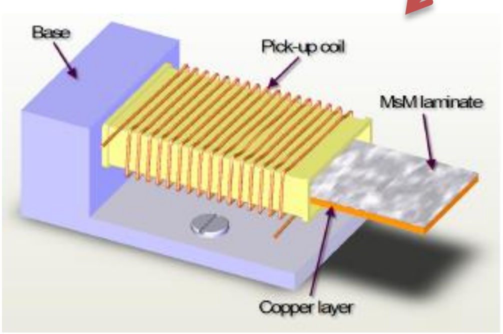

Piezoelectric

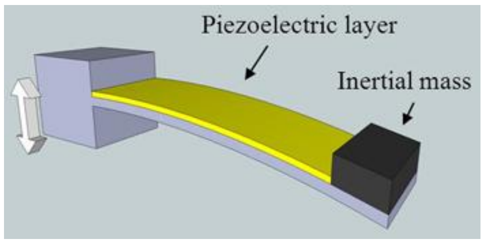

Piezoelectric conversion

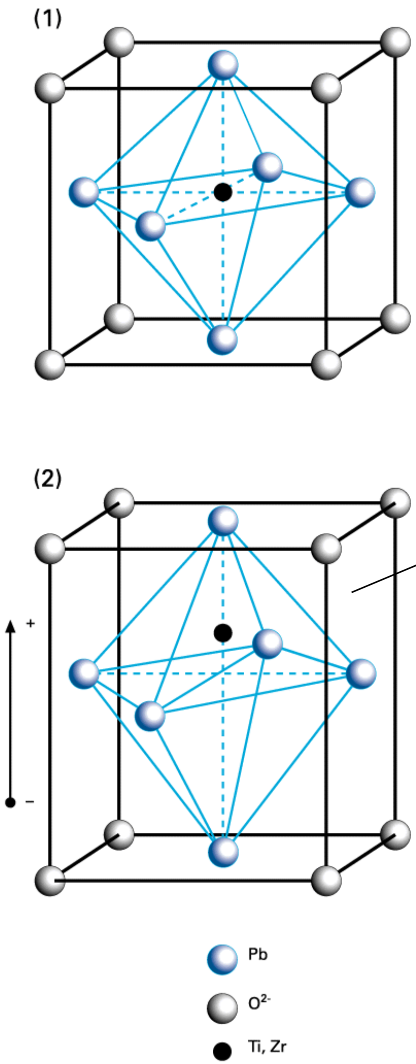

Unpolarized Crystal

Polarized Crystal

Pioneering work on the direct piezoelectric effect (stress-charge) in this material was presented by Jacques and Pierre Curie in 1880

In 1903 Pierre received the Nobel Prize in Physics with his wife, Marie Skłodowska-Curieand and Henri Becquerel, for the research on the radiation phenomena discovered by Professor Henri Becquerel.

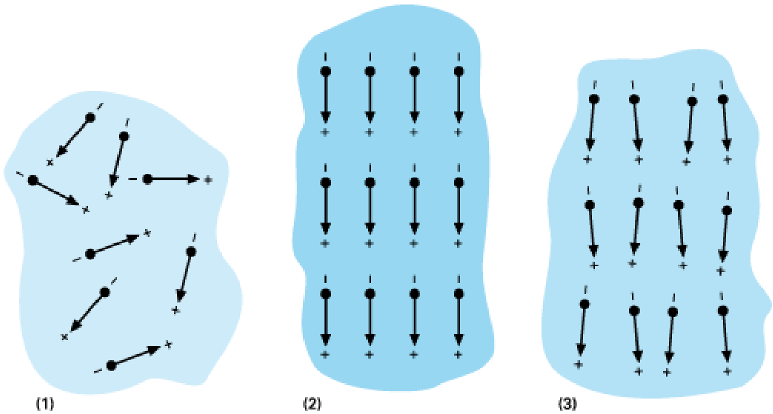

After poling the zirconate-titanate atoms are off center. The molecule becomes elongated and polarized

Piezoelectric conversion

Stress-to-charge conversion

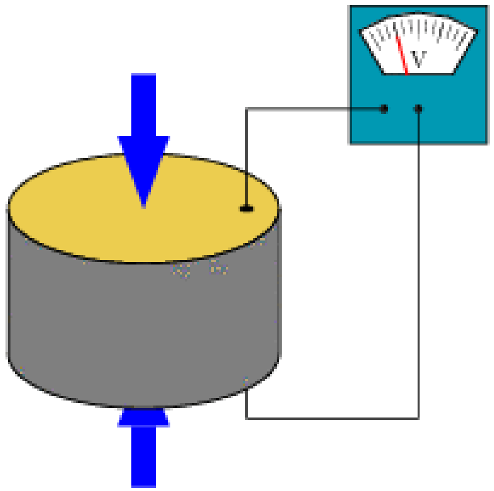

direct piezoelectric effect

Biological

- Bones
- DNA !!!

Naturally-occurring crystals

- Berlinite ($AlPO_4$), a rare phosphate mineral that is structurally identical to quartz
- Cane sugar
- Quartz (SiO_2)
- Rochelle salt

Man-made ceramics

- Barium titanate ($BaTiO_3$)—Barium titanate was the first piezoelectric ceramic discovered.
- Lead titanate ($PbTiO_3$)
- Lead zirconate titanate ($Pb[Zr_xTi_{1-x}]O_3$ $0 \le x \le 1$)—more commonly known as ***PZT***, lead zirconate titanate is the most common piezoelectric ceramic in use today.
- Lithium niobate ($LiNbO_3$)

Polymers

- Polyvinylidene fluoride (PVDF): exhibits piezoelectricity several times greater than quartz. Unlike ceramics, long-chain molecules attract and repel each other when an electric field is applied.

Piezoelectric conversion

33 Mode

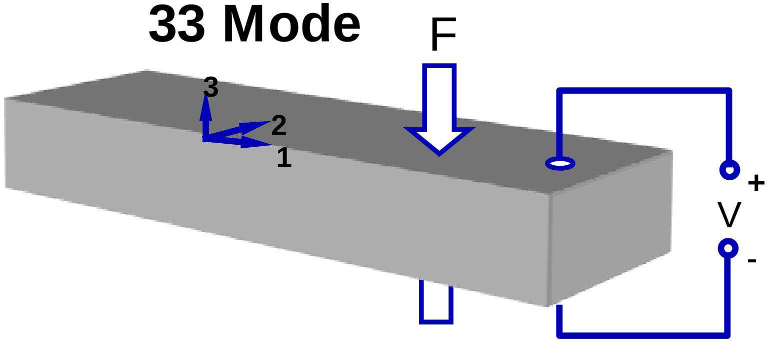

31 Mode

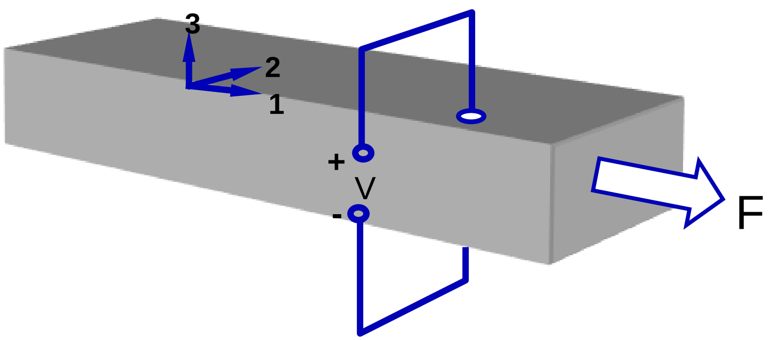

$$S = [s_E]T + [d^t]E$$
$$D = [d]T + [\varepsilon_T]E$$

Strain-charge

$$T = [c^E]S - [e^t]E$$
$$D = [e]S + [\varepsilon^S]E$$

Stress-charge

- S = strain vector (6x1) in Voigt notation
- T = stress vector (6x1) [N/m^2]
- s_E = compliance matrix (6x6) [m^2/N]
- c^E = stifness matrix (6x6) [N/m^2]
- d = piezoelectric coupling matrix (3x6) in Strain-Charge [C/N]
- D = electrical displacement (3x1) [C/m^2]
- e = piezoelectric coupling matrix (3x6) in Stress-Charge [C/m^2]
- ε = electric permittivity (3x3) [F/m]
- E = electric field vector (3x1) [N/C] or [V/m]

Piezoelectric conversion

Characteristic	PZT-5H	BaTiO3	PVDF	AlN (thin film)
d_{33} (10^{-10} C/N)	593	149	-33	5,1
d_{31} (10^{-10} C/N)	-274	78	23	-3,41
k_{33}	0,75	0,48	0,15	0,3
k_{31}	0,39	0,21	0,12	0,23
ε_r	3400	1700	12	10,5

$$k_{31}^2 = \frac{El.energy}{Mech.energy} = \frac{d_{31}^2}{s_{11}^E \varepsilon_{33}^T}$$

Electromechanical Coupling is an adimensional factor that provides the effectiveness of a piezoelectric material. IT's defined as the ratio between the mechanical energy converted and the electric energy input or the electric energy converted per mechanical energy input

Basic model of VEH

zinc oxide (ZnO) nanowires
Wang et al. 2008

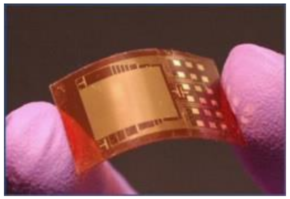

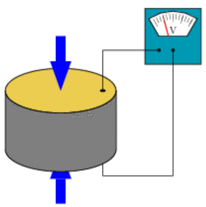

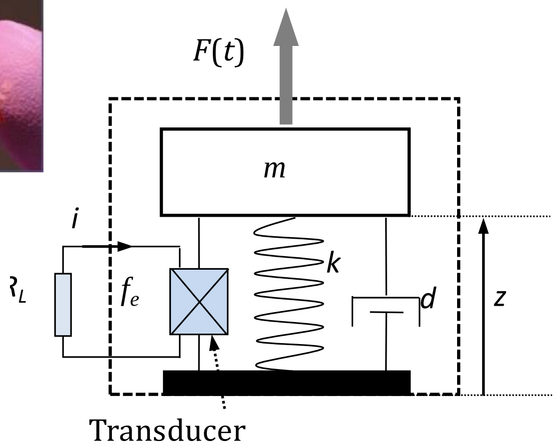

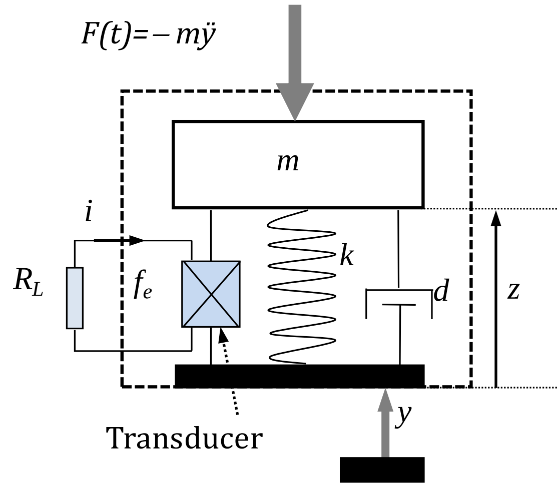

Energy harvesting from moth vibrations
Chang. MIT 2013

Energy Harvesting from dancing

Inertial generators require only one point of attachment to a moving structure, allowing a greater degree of miniaturization.

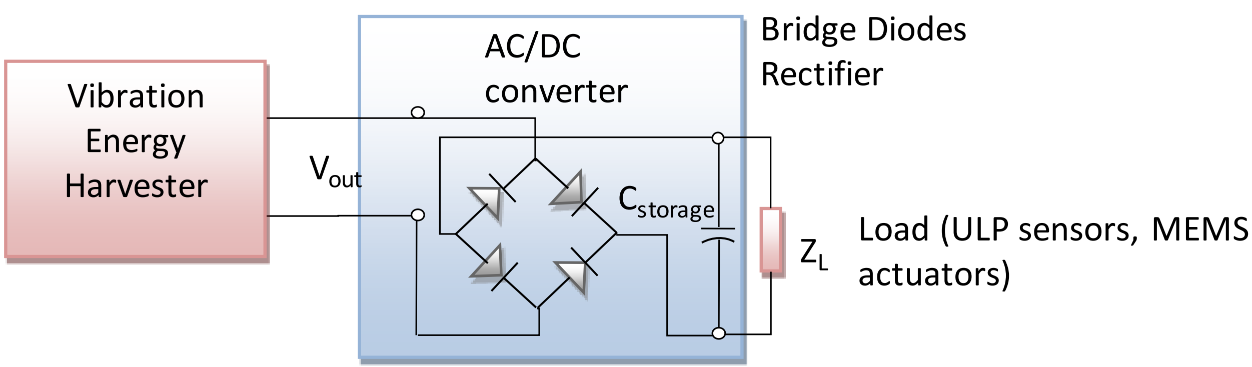

Piezoelectric conversion

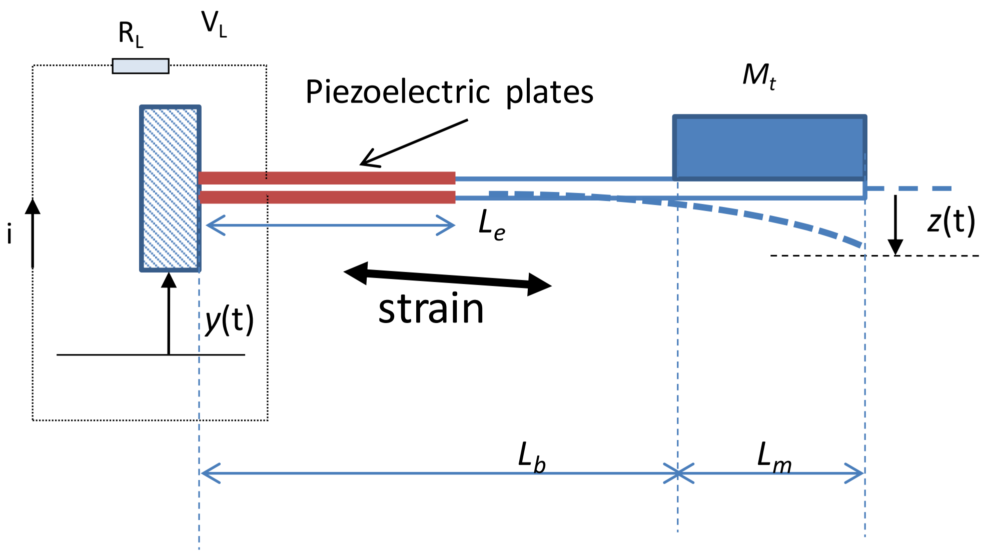

Governing equations

$$\begin{cases} m\ddot{z} + d\dot{z} + kz + \alpha V_L = -m\ddot{y} \\ \dot{V}_L + (\omega_c + \omega_i)V_L = \lambda \omega_c \dot{z} \end{cases}$$

$$\alpha = kd_{31} / h_p k_2, \qquad \lambda = \alpha R_L,$$

$$\omega_c = 1 / R_L C_p, \qquad \omega_i = 1 / R_i C_p,$$

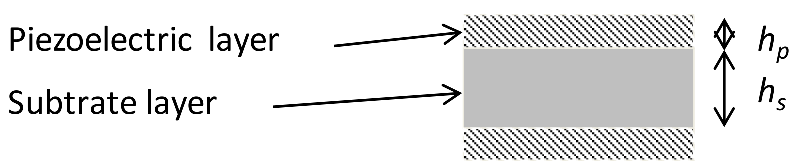

Ep and *Es* are the Young's modulus of piezo layer and steel substrate respectively

$$k = k_1 k_2 E_p,$$

$$k_1 = \frac{2I}{b(2l_b + l_m - l_e)}, \qquad k_2 = \frac{3b(2l_b + l_m - l_e)}{l_b^{\,2}\left(2l_b + \frac{3}{2} l_m\right)},$$

$$b = \frac{h_s + h_p}{2}, \qquad I = 2\left[\frac{w_b h_p^3}{12} + w_b h_p b^2\right] + \frac{E_s / E_p w_b h_s^3}{12},$$

Electromagnetic conversion

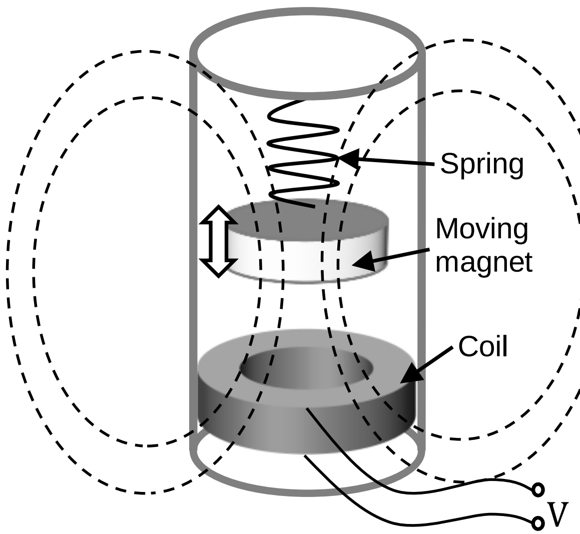

Model

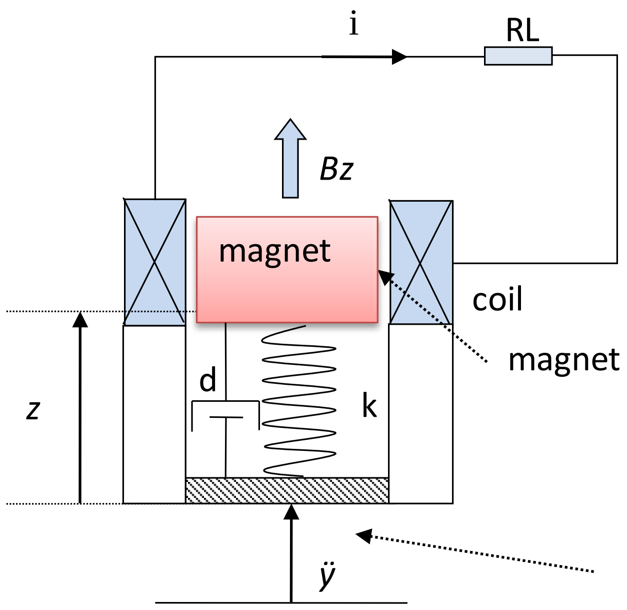

Electromagnetic conversion

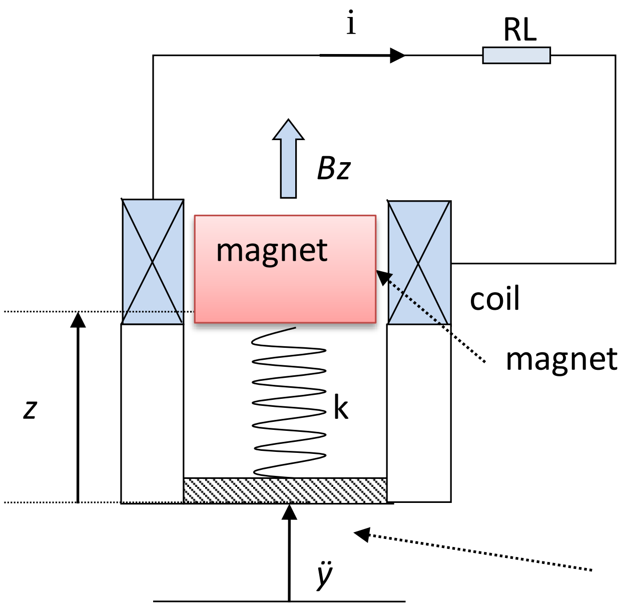

Equivalent circuit

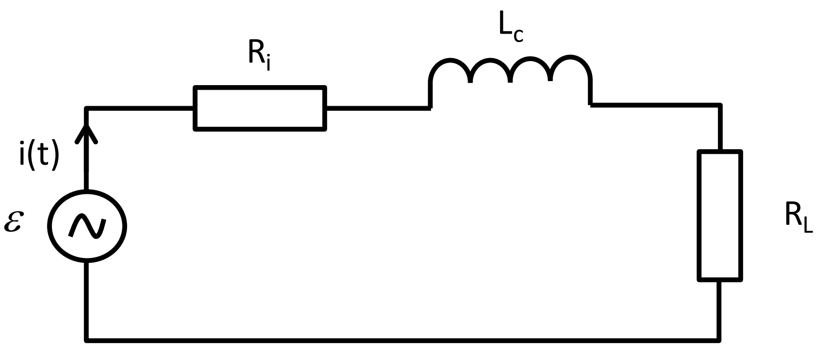

Governing equations

$$\begin{cases} m\ddot{z} + d\dot{z} + kz + \alpha V_L = -m\ddot{y} \\ \dot{V}_L + (\omega_c + \omega_i)V_L = \lambda\omega_c\dot{z} \end{cases}$$

$$\alpha = Bl / R_L, \qquad \lambda = Bl = \alpha R_L,$$

$$\omega_c = R_L / L_c, \qquad \omega_i = R_i / L_c,$$

Electrostatic conversion

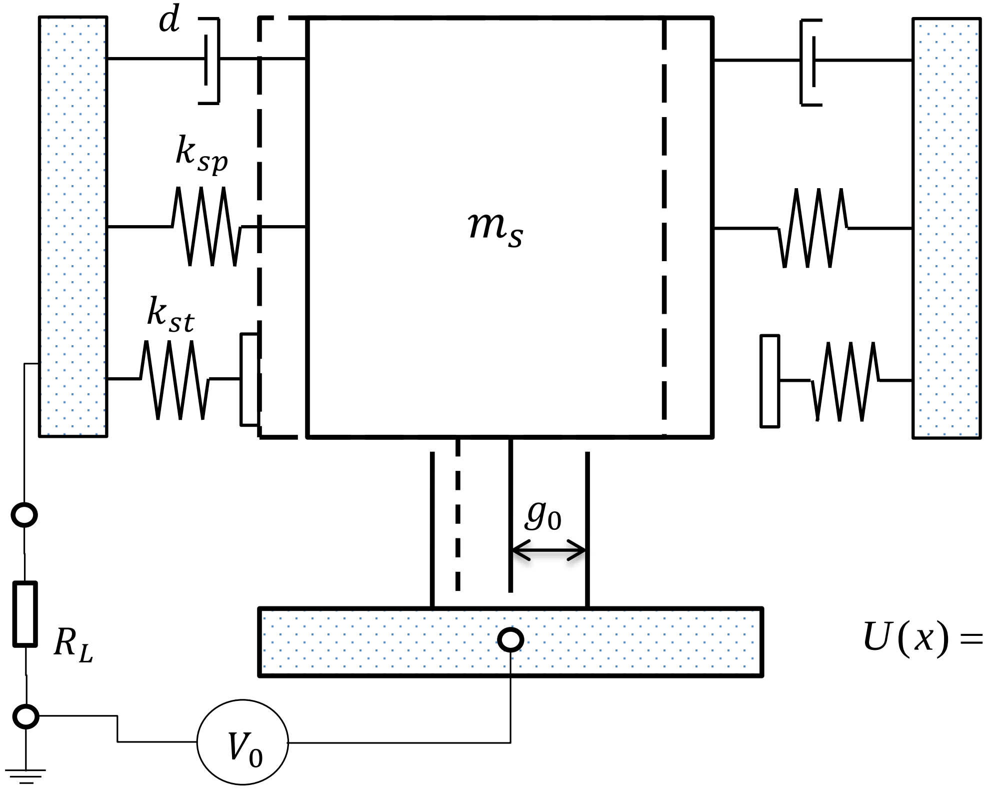

Governing equations

$$m\frac{d^2x}{dt^2}+\left(c_a+c_i\right)\frac{dx}{dt}+\frac{dU(x)}{dx}=-m\frac{d^2y}{dt^2},$$

$$R_L\frac{d}{dt}(C\cdot V)+V=U_0,$$

$$U(x)=\begin{cases}\frac{1}{2}k_{sp}x^2-\frac{1}{2}C(x)U_0^2, & \text{for } |x|<x_{\lim}\\ \frac{1}{2}(k_{sp}+k_{st})x^2-\frac{1}{2}C(x)U_0^2, & \text{for } |x|\geq x_{\lim}\end{cases}$$

Electrostatic conversion

MEMS e-VEH

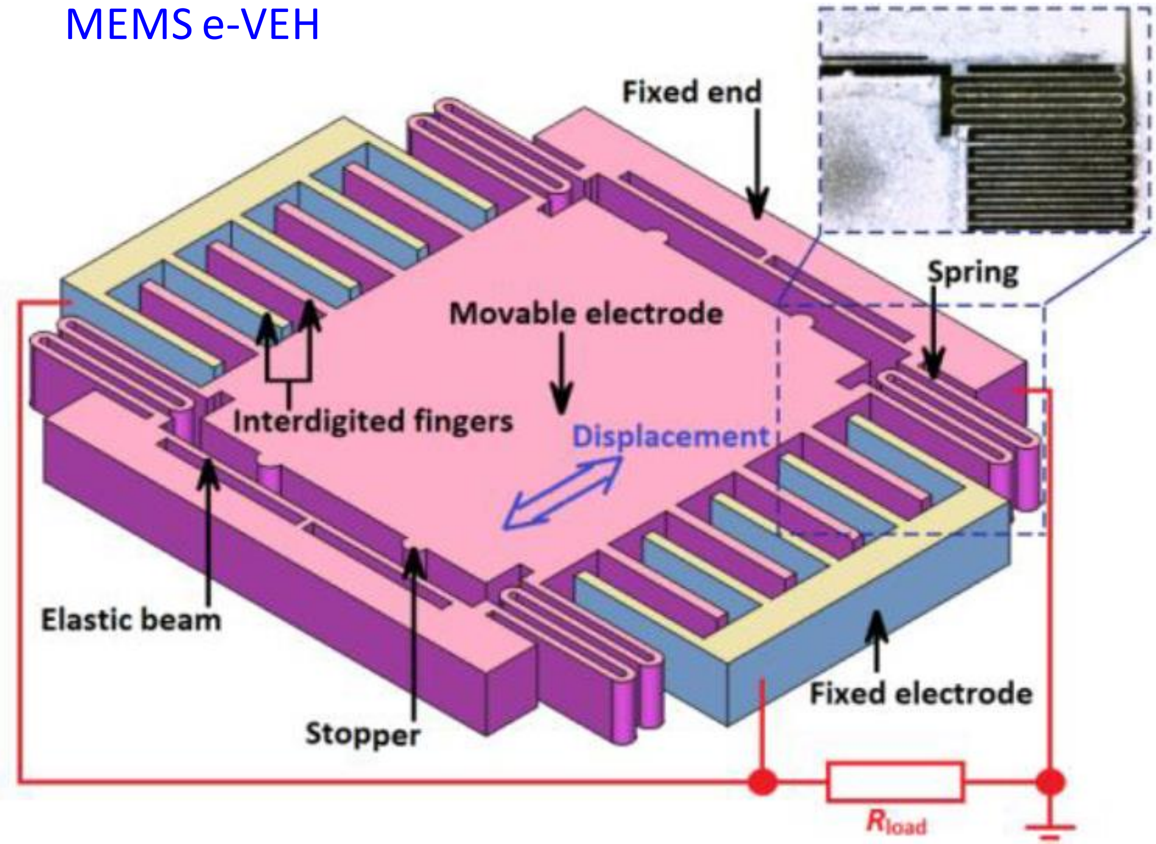

Y. Lu, F. Cottone, S. Boisseau, F. Marty, D. Galayko, and P. Basset, *Applied Physics Letters* 2015.

General model

Electromagnetic transduction **Piezoelectric transduction**

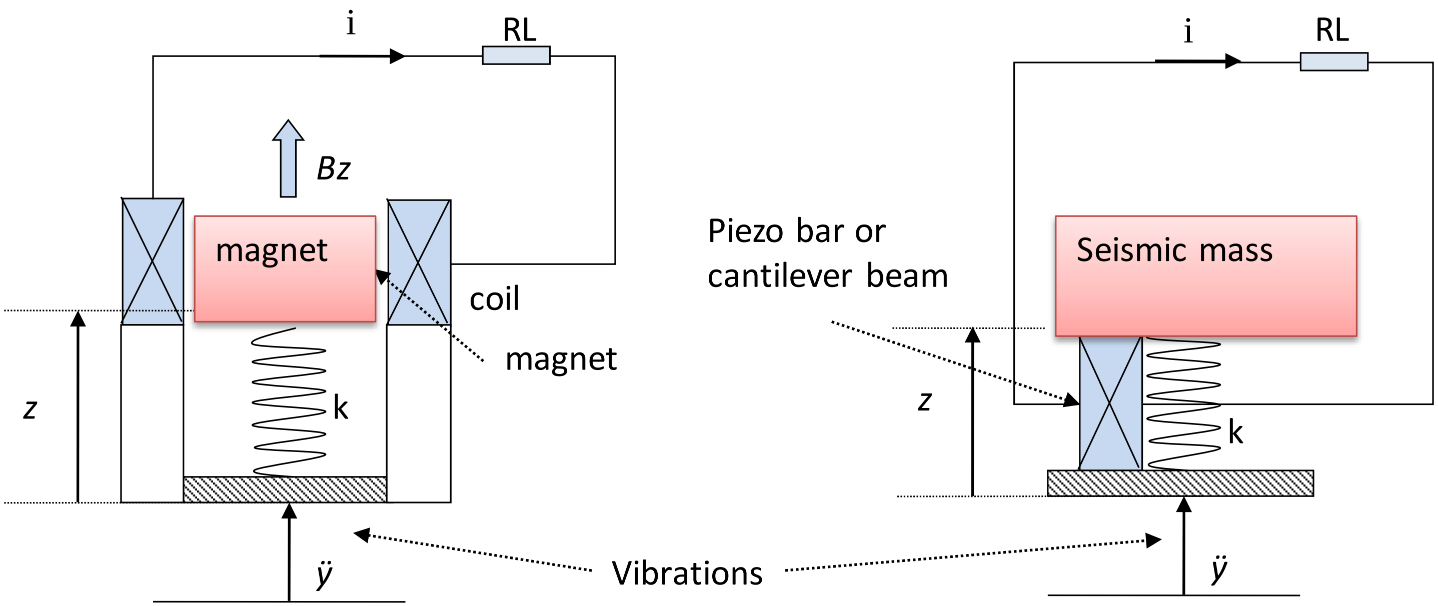

$$\begin{cases} m\ddot{z} + d\dot{z} + \dfrac{dU(z)}{dz} + \alpha V_L = -m\ddot{y} \\ \dot{V}_L + (\omega_c + \omega_i)V_L = \lambda\omega_c\dot{z} \end{cases}$$

$\alpha, \lambda, \omega_c, \omega_i$

Depends on the specific transduction technique!

General model

For LINEAR mechanical oscillators

$$\begin{cases} m\ddot{z} + d\dot{z} + kz + \alpha V_L = -m\ddot{y} \\ \dot{V}_L + (\omega_c + \omega_i) V_L = \lambda \omega_c \dot{z} \end{cases}$$

Laplace transform

$$\ddot{y} = Y_0 e^{j\omega t}$$

$$\begin{pmatrix} ms^2 + ds + k & \alpha \\ -\lambda\omega_c s & s + \omega_c \end{pmatrix} \begin{pmatrix} Z \\ V \end{pmatrix} = \begin{pmatrix} -mY \\ 0 \end{pmatrix}$$

$$Z = \frac{-mY}{\det A}(s+\omega_c) = \frac{-mY \cdot (s+\omega_c)}{ms^3 + (m\omega_c + d)s^2 + (k + \alpha\lambda\omega_c + d\omega_c)s + k\omega_c},$$

$$V = \frac{-mY}{\det A}\lambda\omega_c s = \frac{-mY \cdot \lambda\omega_c s}{ms^3 + (m\omega_c + d)s^2 + (k + \alpha\lambda\omega_c + d\omega_c)s + k\omega_c}.$$

Hence, the transfer functions between displacement and voltage over input acceleration are given by

$$H_{ZY}(s) = \frac{Z}{Y}, \quad \text{(a)} \qquad H_{VY}(s) = \frac{V}{Y}. \quad \text{(b)}$$

By substituting s=jω in , we can calculate the electrical power dissipated across the resistive load

$$P_e(\omega) = \frac{Y_0^2}{2R_L} \left| \frac{m_2 \lambda \omega_c j\omega}{(\omega_c + j\omega)(-m_2\omega^2 + d_2 j\omega + k_2) + \alpha\lambda\omega_c j\omega} \right|^2$$

Comparison of conversion techniques

Technique	Advantages	Drawbacks
Piezoelectric	• high output voltages • well adapted for miniaturization • high coupling in single crystal • no external voltage source needed	• expensive • small coupling for piezoelectric thin films • large load optimal impedance required (MΩ) • Fatigue effect
Electrostatic	• suited for MEMS integration • good output voltage (2-10V) • possiblity of tuning electromechanical coupling • Long-lasting	• need of external bias voltage • relatively low power density at small scale
Electromagnetic	• good for low frequencies (5-100Hz) • no external voltage source needed • suitable to drive low impedances	• inefficient at MEMS scales: low magnetic field, micro-magnets manufacturing issues • large mass displacement required.

Main limits of resonant VEHs

- narrow bandwidth that implies constrainec resonant frequency-tuned applications
- Non-adaptation to variable vibration sources
- small inertial mass and high resonant frequency at micro/nano-scale -> most of vibration sources are below 100 Hz

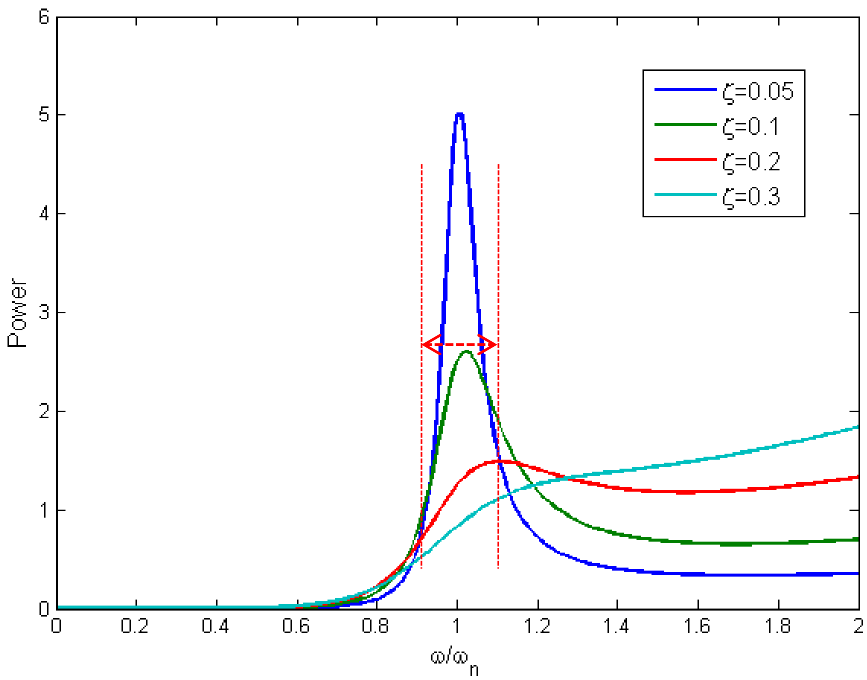

At 20% off the resonance the power falls by 80-90%

Beyond linear harvesting systems

Frequency tuning

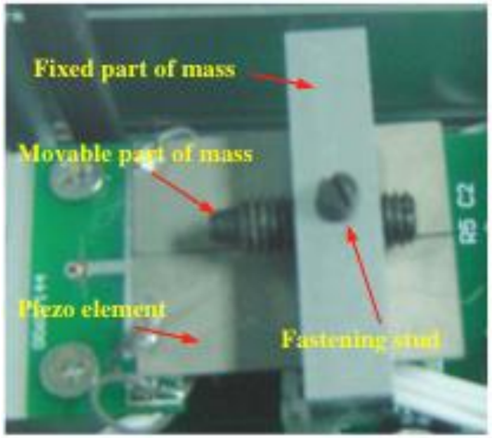

Piezoelectric cantilever with a movable mass

Wu et al. 2008

Piezoelectric cantilever with magnetic tuning

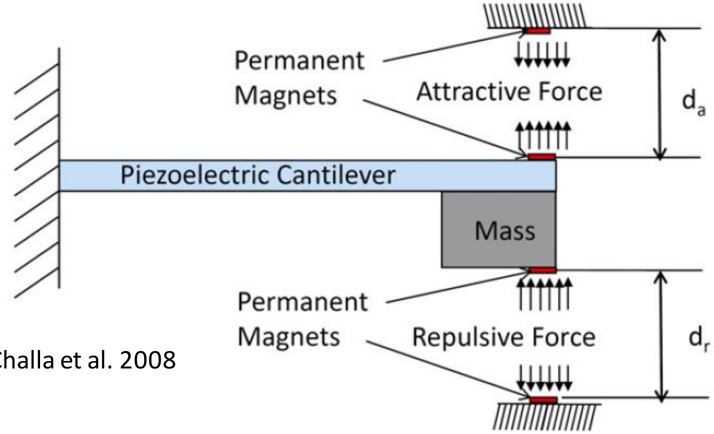

Challa et al. 2008

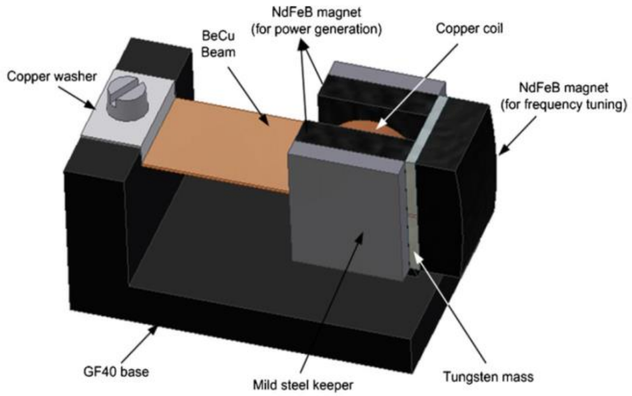

Zhu, et al. (2010). *Sensors and Actuators A: Physical*

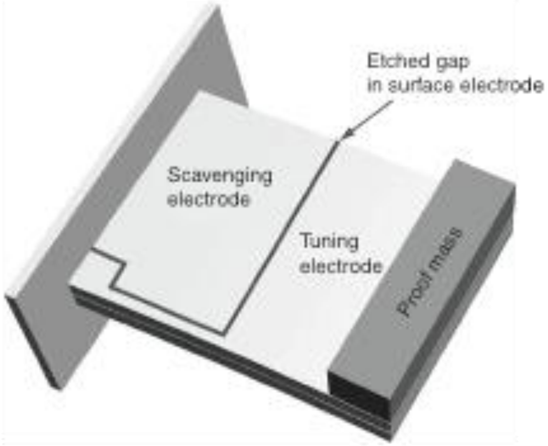

Piezoelectric beam with a scavenging and a tuning part

Roundy and Zhang 2004

Beyond linear harvesting systems

Multimodal Energy Harvesting

Tadesse et al. 2009

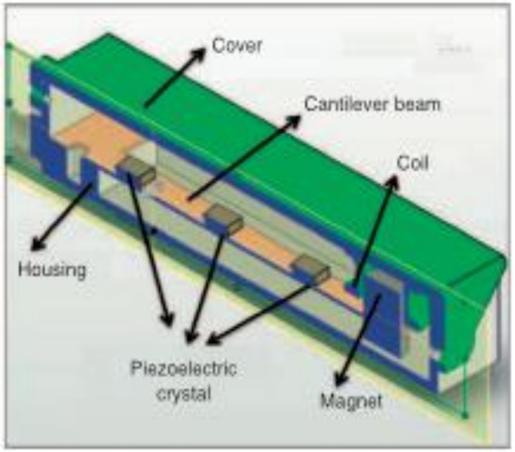

Hybrid harvester with piezoelectric and electromagnetic transduction mechanisms

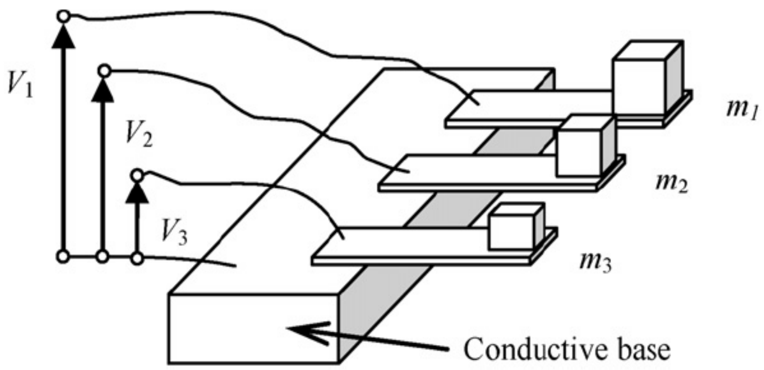

Ferrari, M., et al. (2008). *Sensors and Actuators A: Physical*

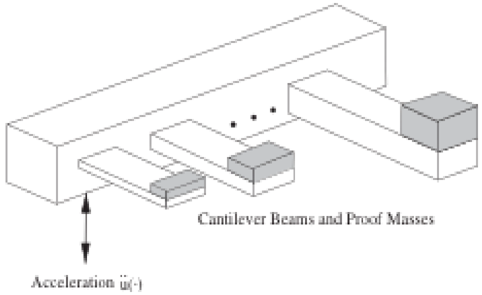

Shahruz 2006

Piezoelectric cantilever arrays with various lengths and tip masses

Beyond linear harvesting systems

Frequency-up conversion

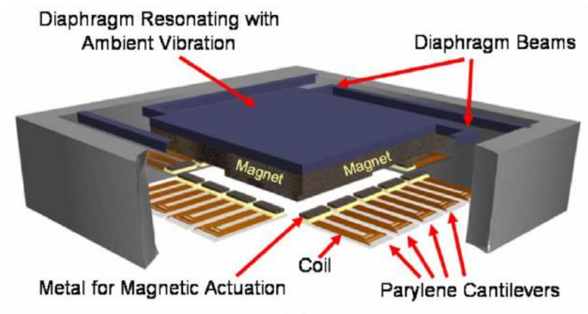

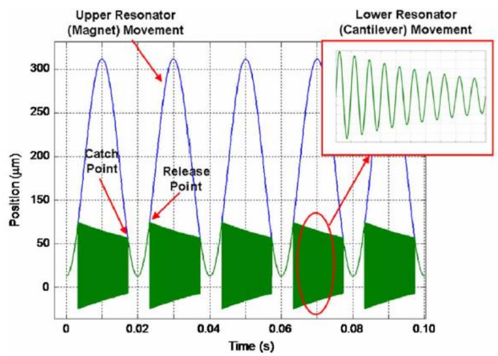

H. Kulah and K. Najafi, IEEE Sensors Journal **8** (3), 261 (2008).

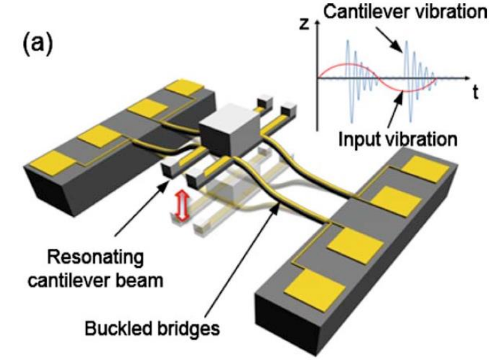

Jung, S.-M. et al. (2010). *Applied Physics Letters*

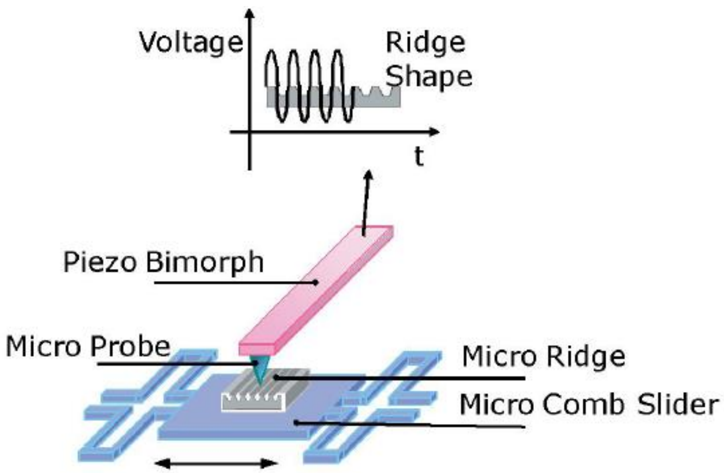

D.G. Lee et al. IEEE porc. (2007)

Impact electrostatic MEMS generator

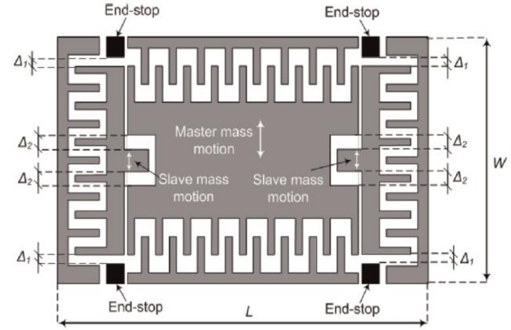

Le, C. P., Halvorsen (2012). *Journal of Intelligent Material Systems and Structures*

Beyond linear harvesting systems

Nonlinear systems for vibration energy harvesting

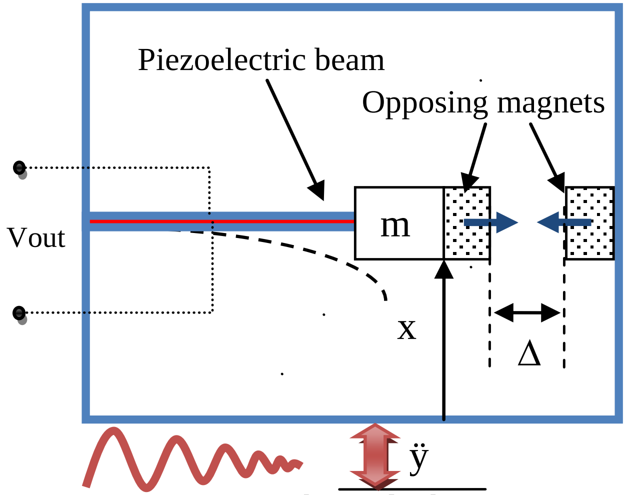

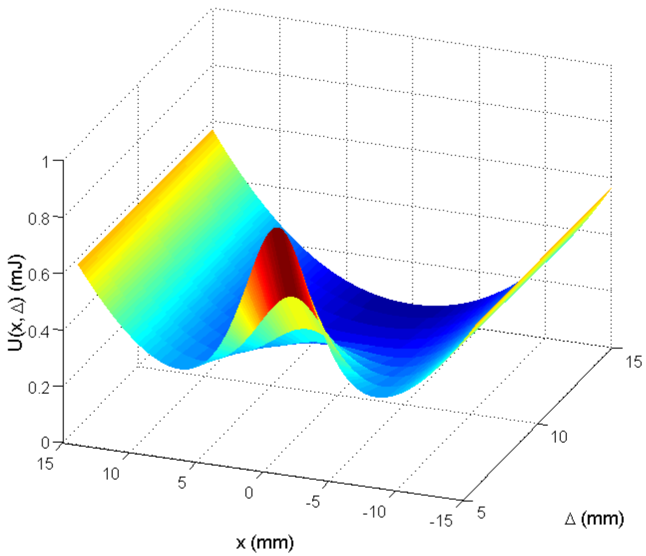

Magneto-elastic potential

$$U(x,\Delta)=\frac{1}{2}K_{eff}x^2+\frac{\mu_0}{2\pi}\frac{M_1M_2}{(x^2+\Delta^2)^{3/2}}$$

Governing equations of a single-DOF piezo-magnetoelastic model

$$\begin{cases} m\ddot{x}(t)+\delta\dot{x}(t)+K_{eff}x(t)+\dfrac{\partial U(x,\Delta)}{\partial x}+K_vV(t)=-m\ddot{y}(t) \\ \dot{V}(t)+\dfrac{1}{\tau}V(t)=K_c\dot{x}(t); \qquad \tau=R_LC_p \end{cases}$$

Cottone, F., H. Vocca & L. Gammaitoni. *PRL,* 102 (2009).

Beyond linear harvesting systems

Bistable: inter-well and intra-well oscillations

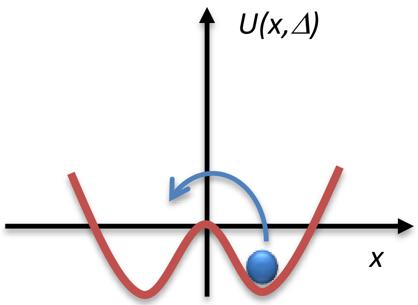

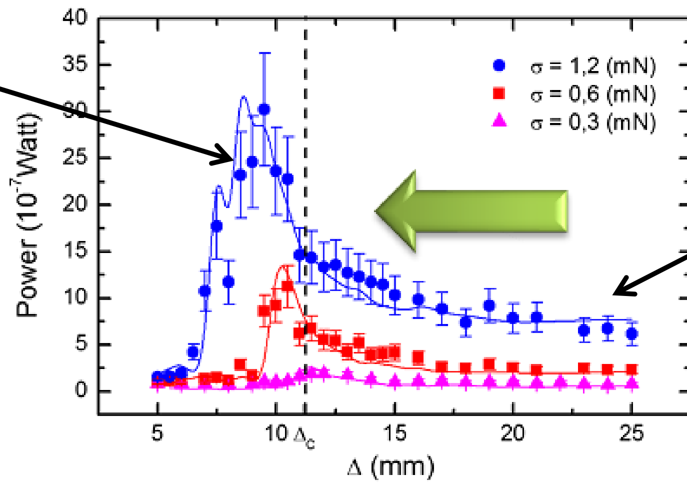

Resonant monostable

Δ=25mm

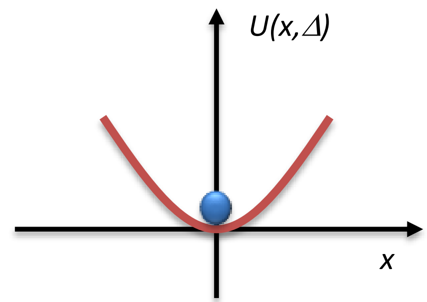

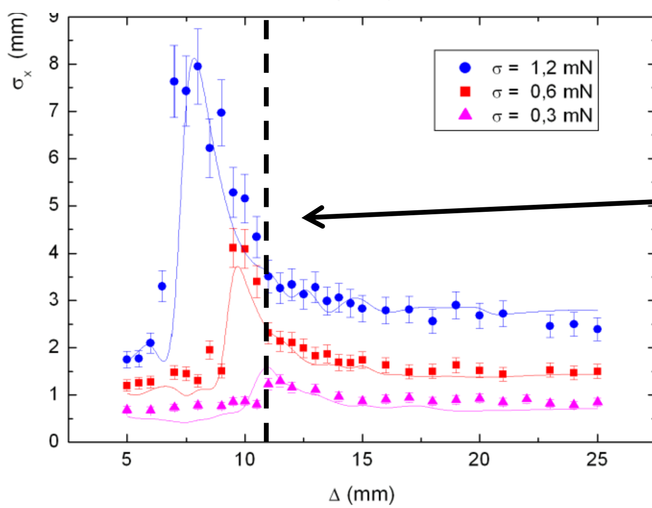

Bifurcation point

Beyond linear harvesting systems

Buckled beam piezoelectric harvesters

Cottone, F., Gammaitoni, L., Vocca, H., Ferrari, M., & Ferrari, V. (2012). *Smart materials and structures, 21*(3), 035021

Snapping between buckled states

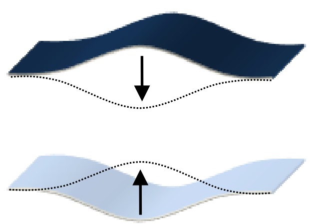

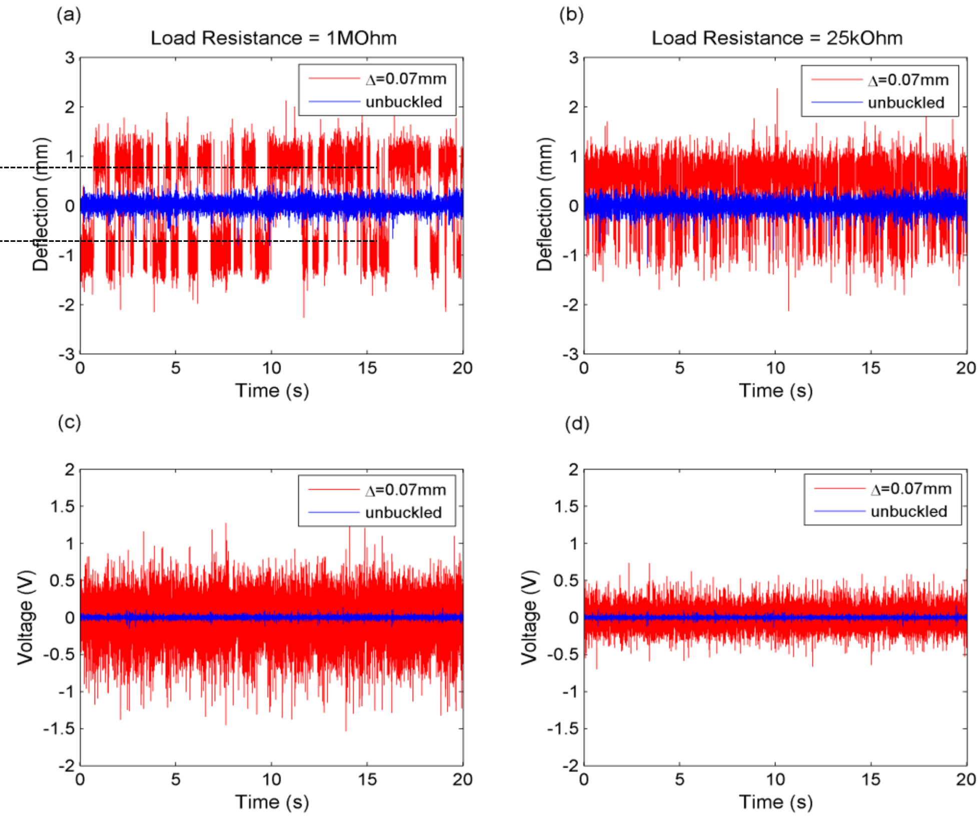

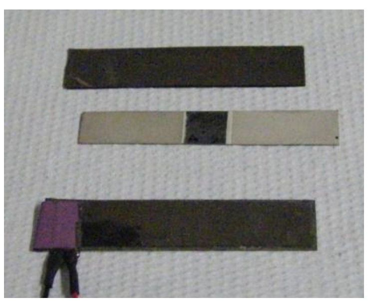

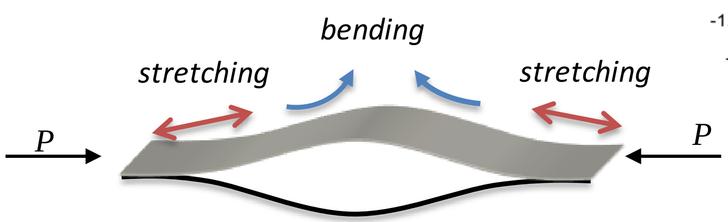

Beyond linear harvesting systems

Experimental and numerical results

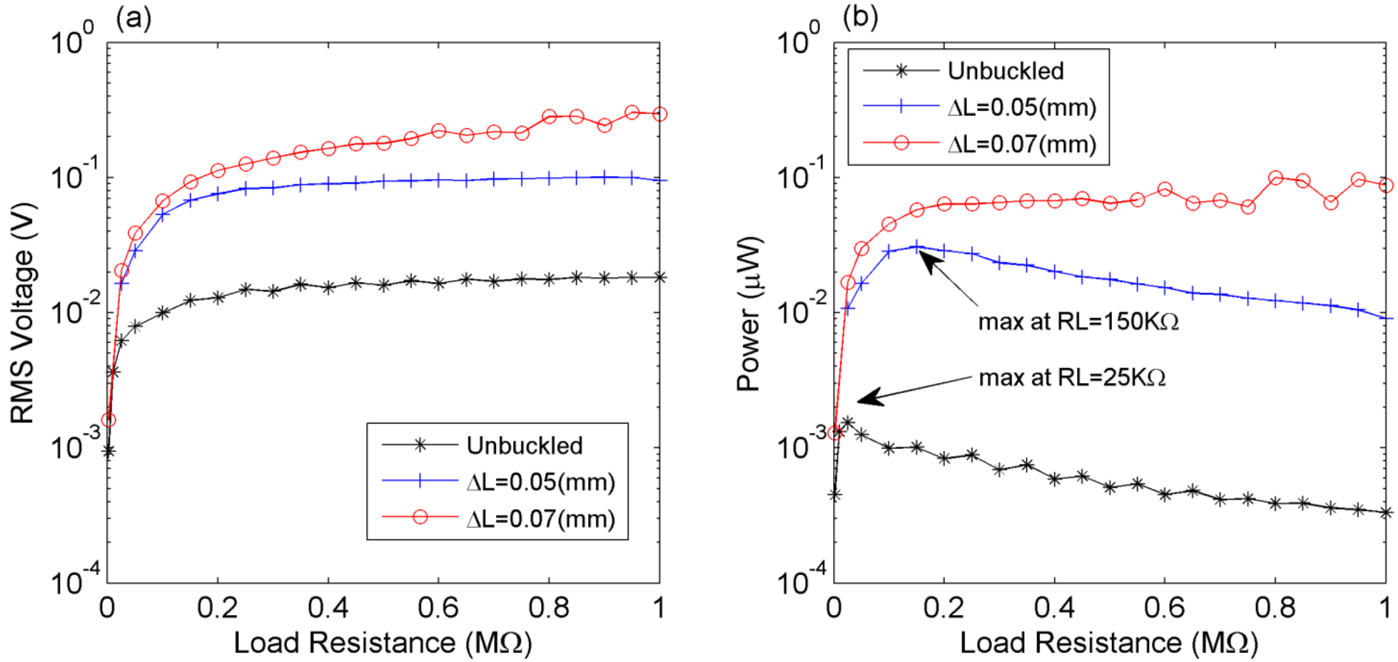

Cottone, F., L. Gammaitoni, H. Vocca, M. Ferrari & V. Ferrari (2012) Smart materials and structures, 21, 2012.

Beyond linear harvesting systems

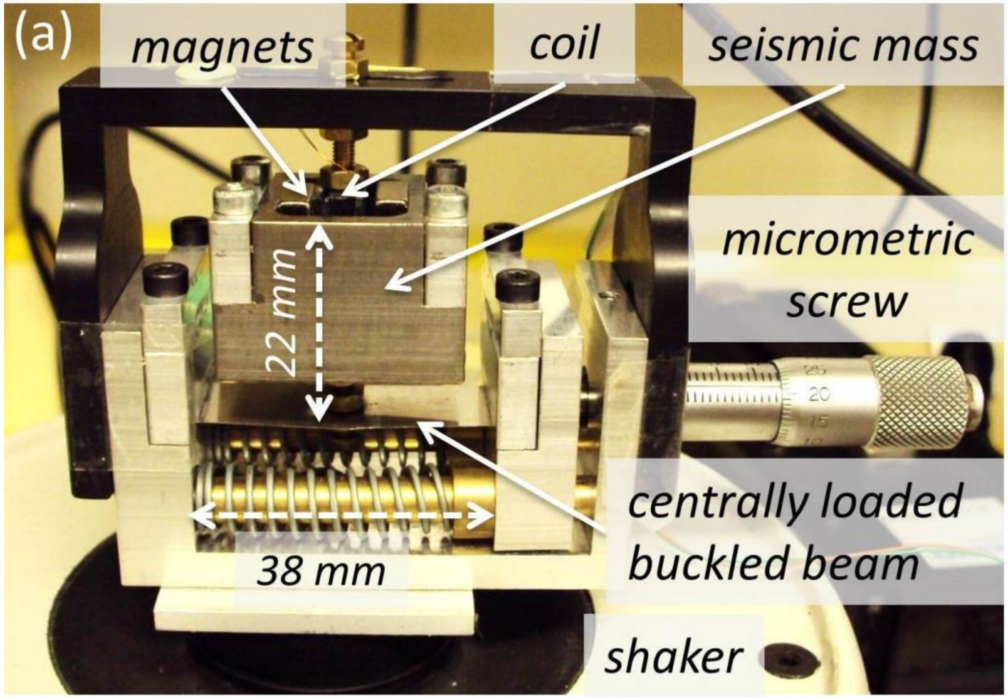

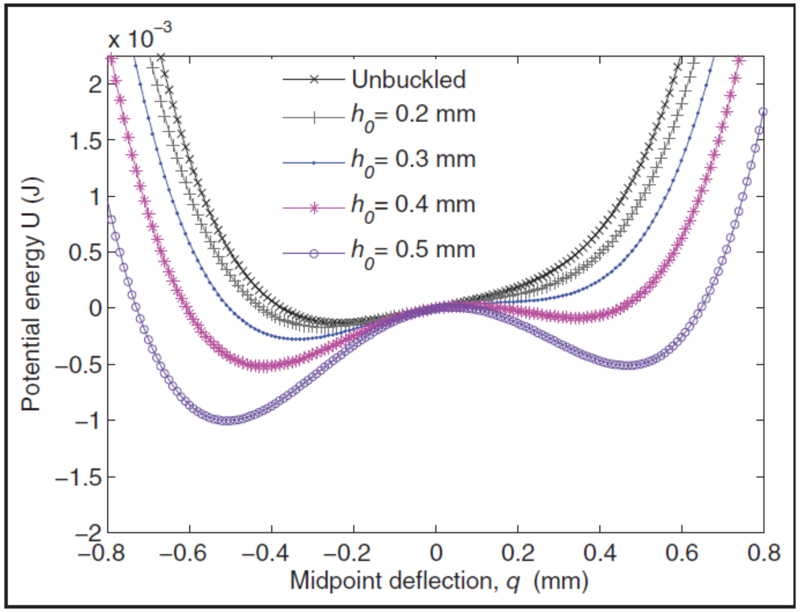

Figure 3. Potential energy of the system for increasing values of buckling height h_0.

F. Cottone et al. *J. Intell. Mater. Syst. Struct.* 2014.

Beyond linear harvesting systems

Bandwidth enhancement of 2.5x with bistability at 0,2 grms

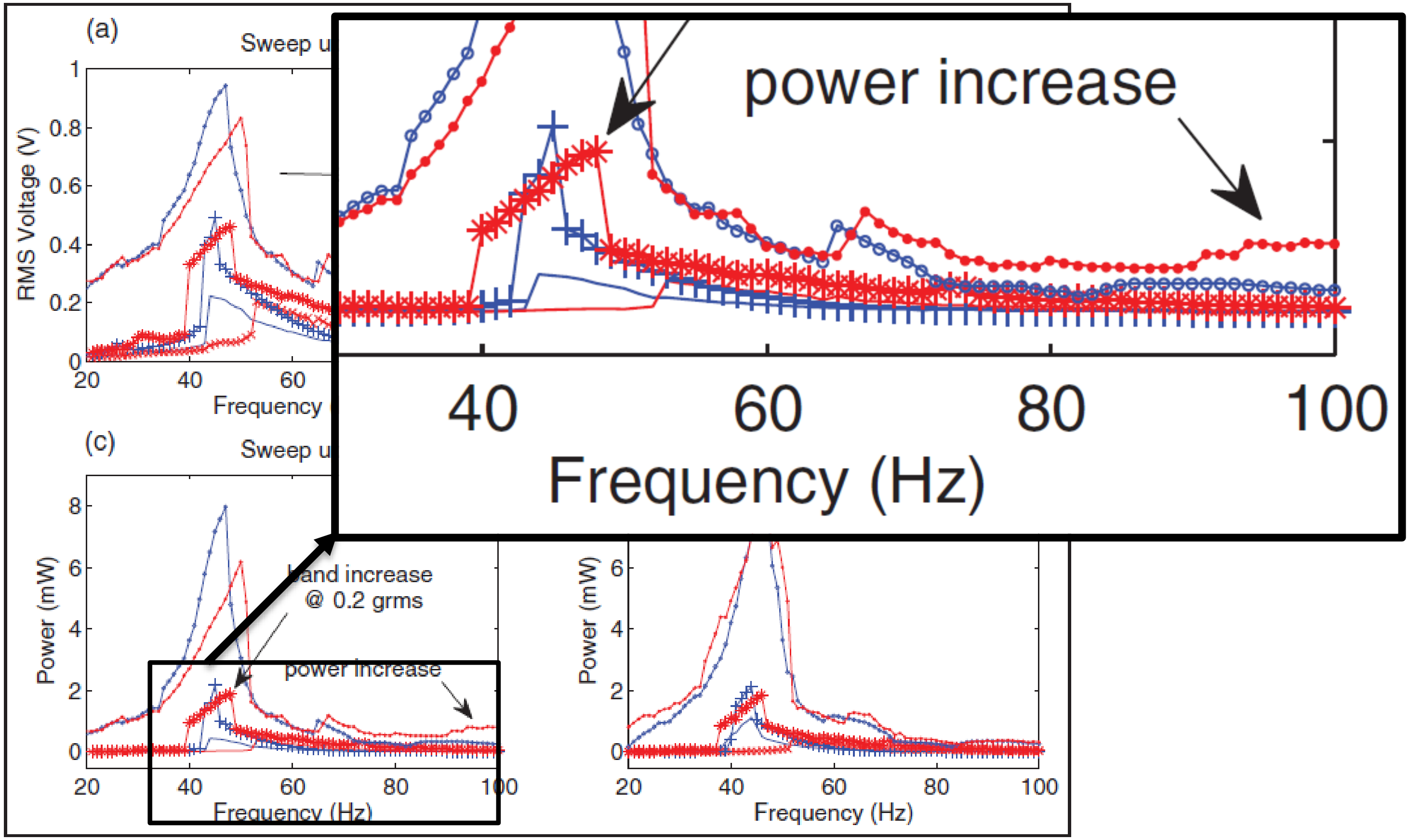

Figure 6. Experimental comparison of unbuckled- and buckled-beam (h_0 = 0.3 mm) generators for up (left column) and down (right column) frequency sweeps with acceleration amplitudes of 0.1, 0.2, and 0.5 g_{rms}. (a and b) *rms* voltage and (c and d) the corresponding power dissipated across the optimal load resistance R_L = 112 Ω.
rms: root mean square.

Figure of Merit

Volume figure of merit

$$\mathrm{FoM_V} = \frac{\text{Useful Power Output}}{\frac{1}{16} Y_0 \rho_{\mathrm{Au}} Vol^{\frac{4}{3}} \omega^3}$$

Bandwidth figure of merit

$$\mathrm{FoM_{BW}} = \mathrm{FoM_V} \times \frac{\delta\omega_{1\ \mathrm{dB}}}{\omega}$$

Frequency range within which the output power is less than 1 dB
below its maximum value

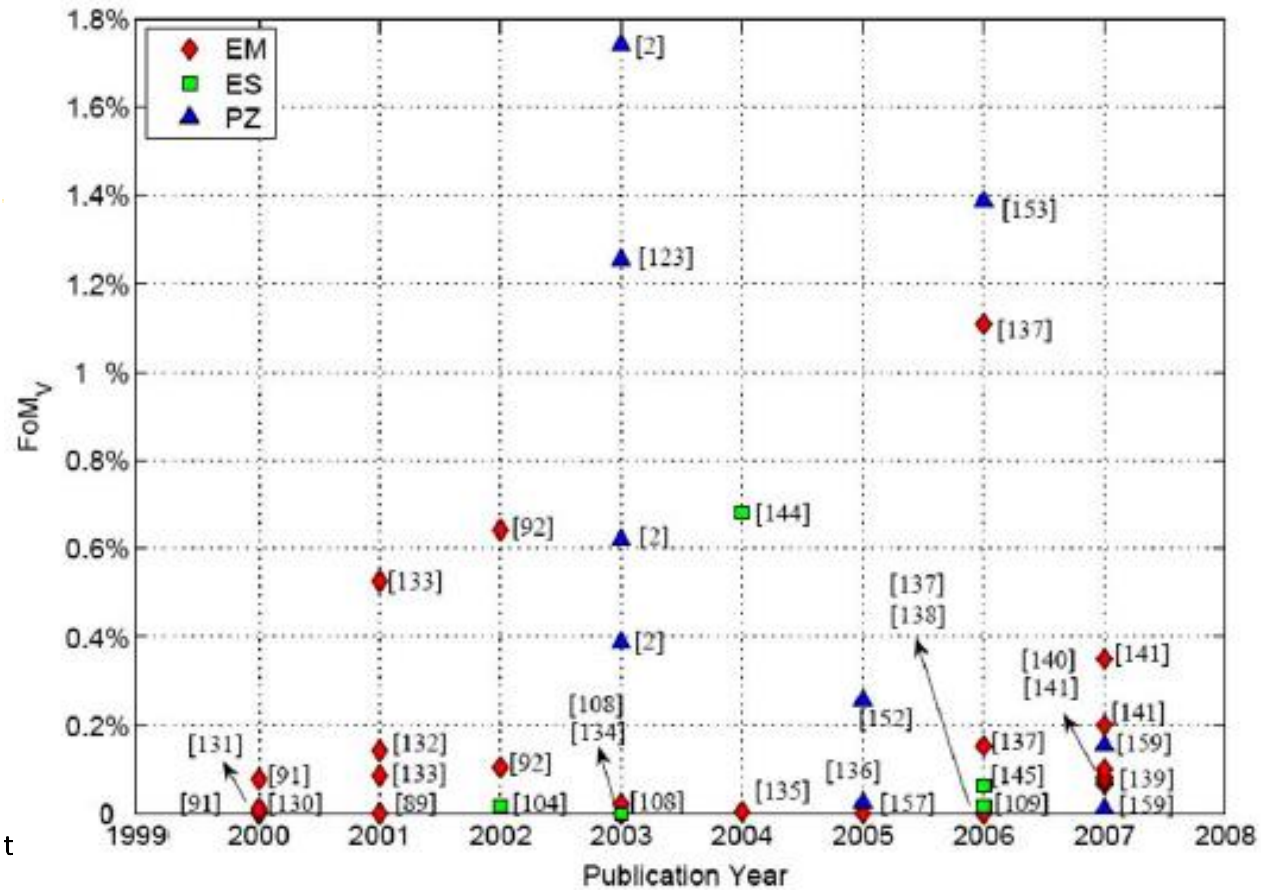

Mitcheson, P. D., E. M. Yeatman, et al. (2008). Proceedings of the IEEE **96**(9): 1457-1486.

Microscale energy harvesters

MEMS-based drug delivery systems

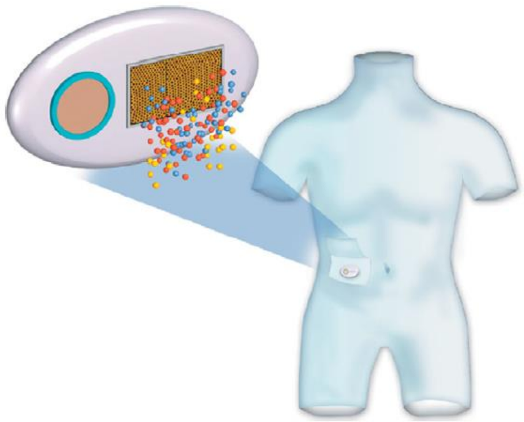

Bohm S. et al. 2000

Body-powered oximeter

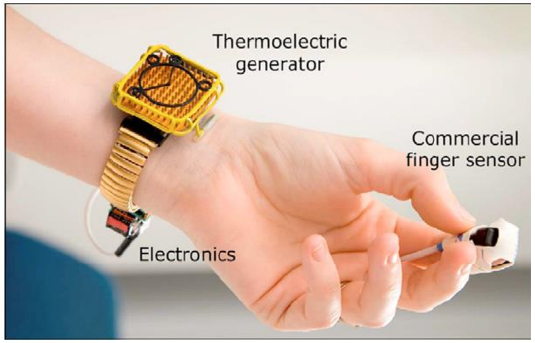

Leonov, V., & Vullers, R. J. (2009).

Heart powered pacemaker

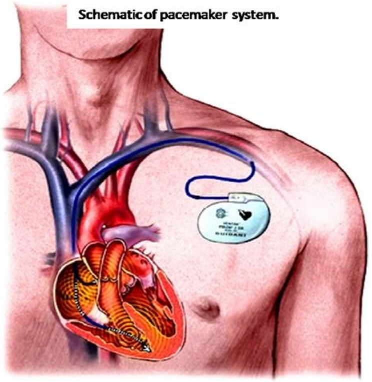

D. Tran, Stanford Univ. 2007

Pacemaker consumption is **40uW**.

Beating heart could produce **200uW** of power

Micro-robot for remote monitoring

A. Freitas Jr., Nanomedicine, Landes Bioscience, 1999

The input power a 20 mg robotic fly is **10 – 100 uW**

Microscale energy harvesters: scaling issues

First order power calculus with William and Yates model

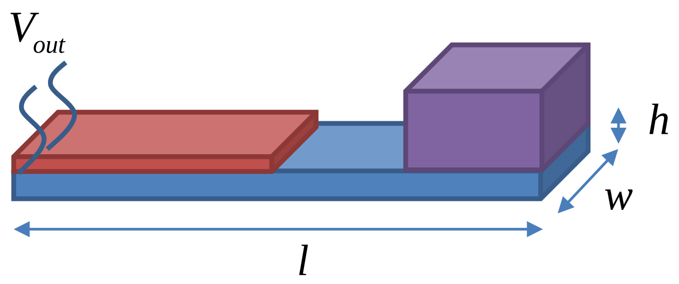

$$\omega_n = 2\pi C_n \sqrt{\frac{E}{\rho}} \frac{h}{l^2}$$

Boudary conditions	C1
doubly clamped	1,03
cantilever	0,162

$$k = \xi \frac{Ewh^3}{l^3}$$

Boudary conditions	Uniform load ξ	Point load ξ
doubly clamped	32	16
cantilever	0,67	0,25

- Low efficiency off resonance
- High resonant frequency at miniature scales
- Power → $A^2 l^4$ where A is the acceleration and l the linear dimension

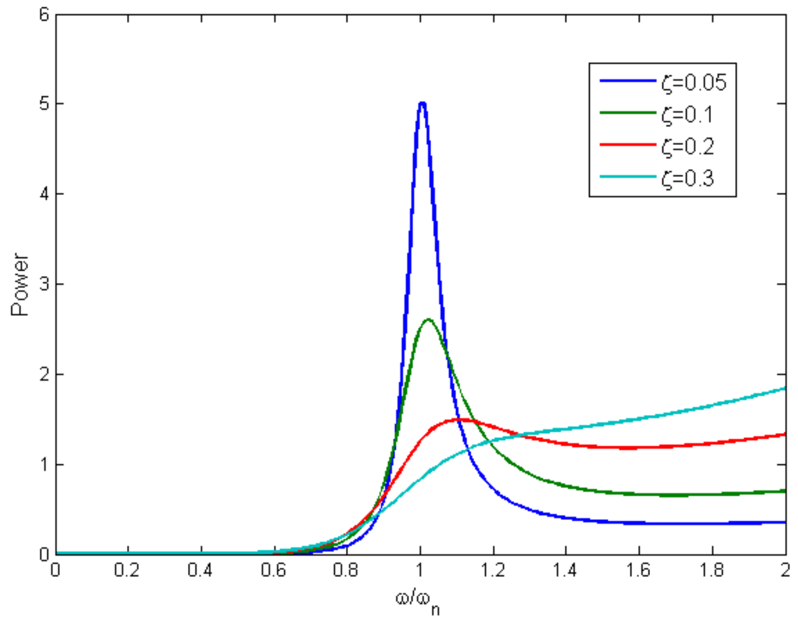

Microscale energy harvesters: scaling issues

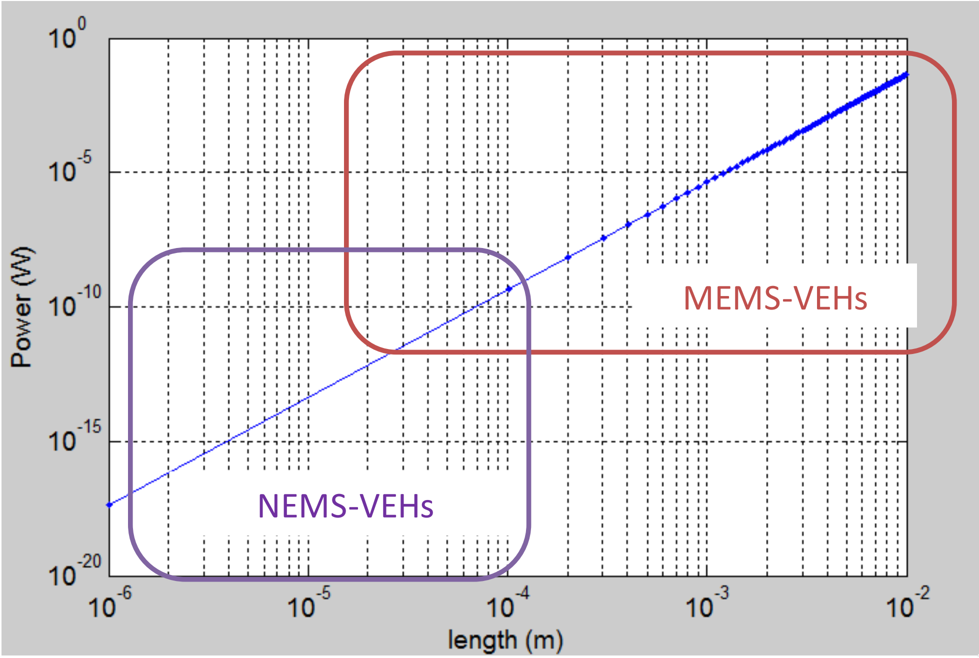

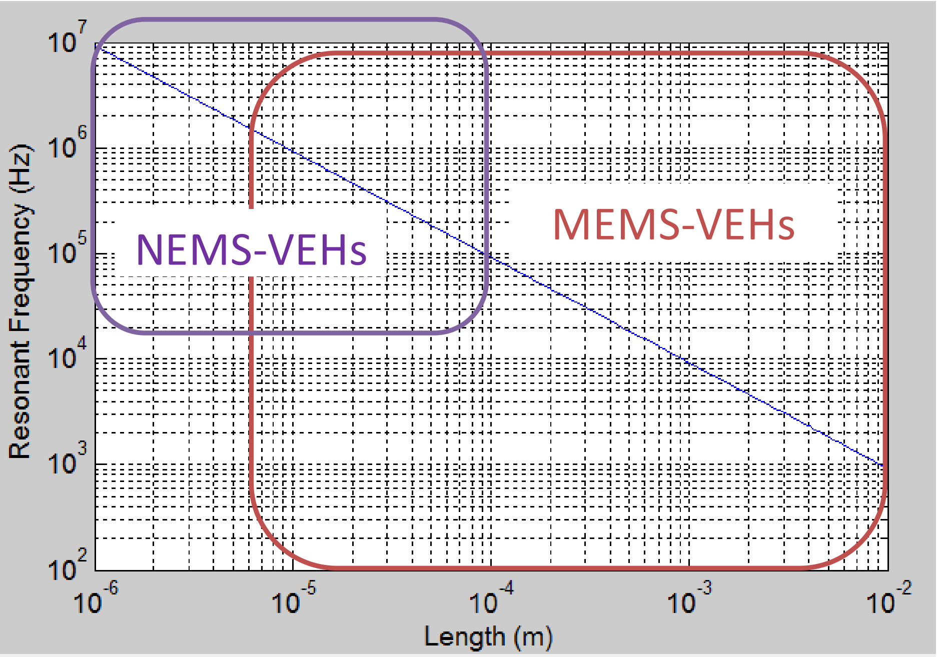

Microscale energy harvesters: scaling issues

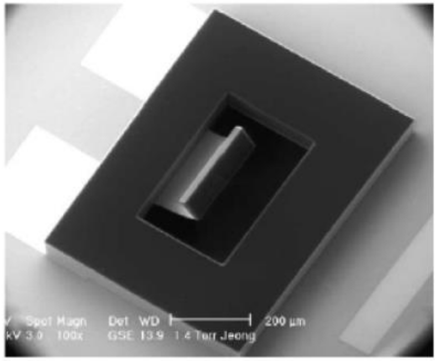

Jeon et al. 2005

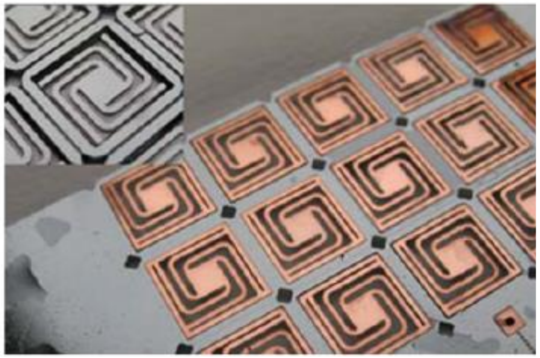

EM generator, Miao et al. 2006

Chang. MIT 2013

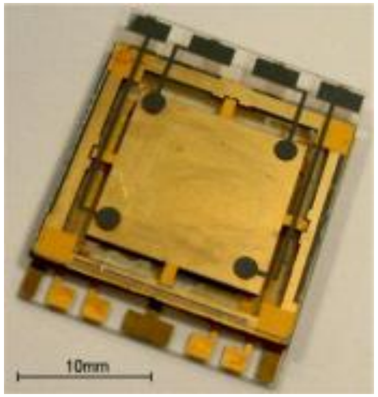

Mitcheson 2005 (UK)
Electrostatic generator 20Hz
2.5uW @ 1g

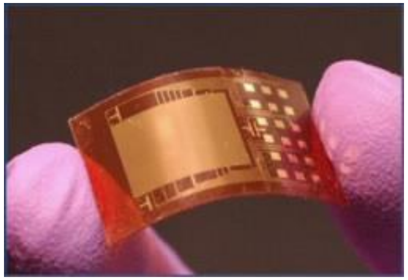

ZnO nanowires
Wang, Georgia Tech (2005)

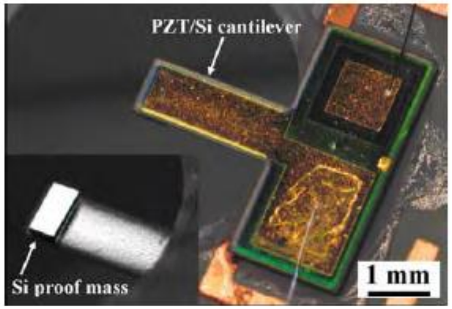

D. Briand, EPFL 2010

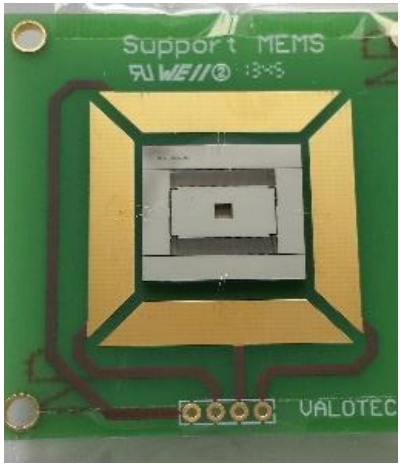

Cottone F., Basset P. ESIEE Paris 2013

2005 2015

Low-frequency MEMS electrostatic VEH

Prototype fabrication process

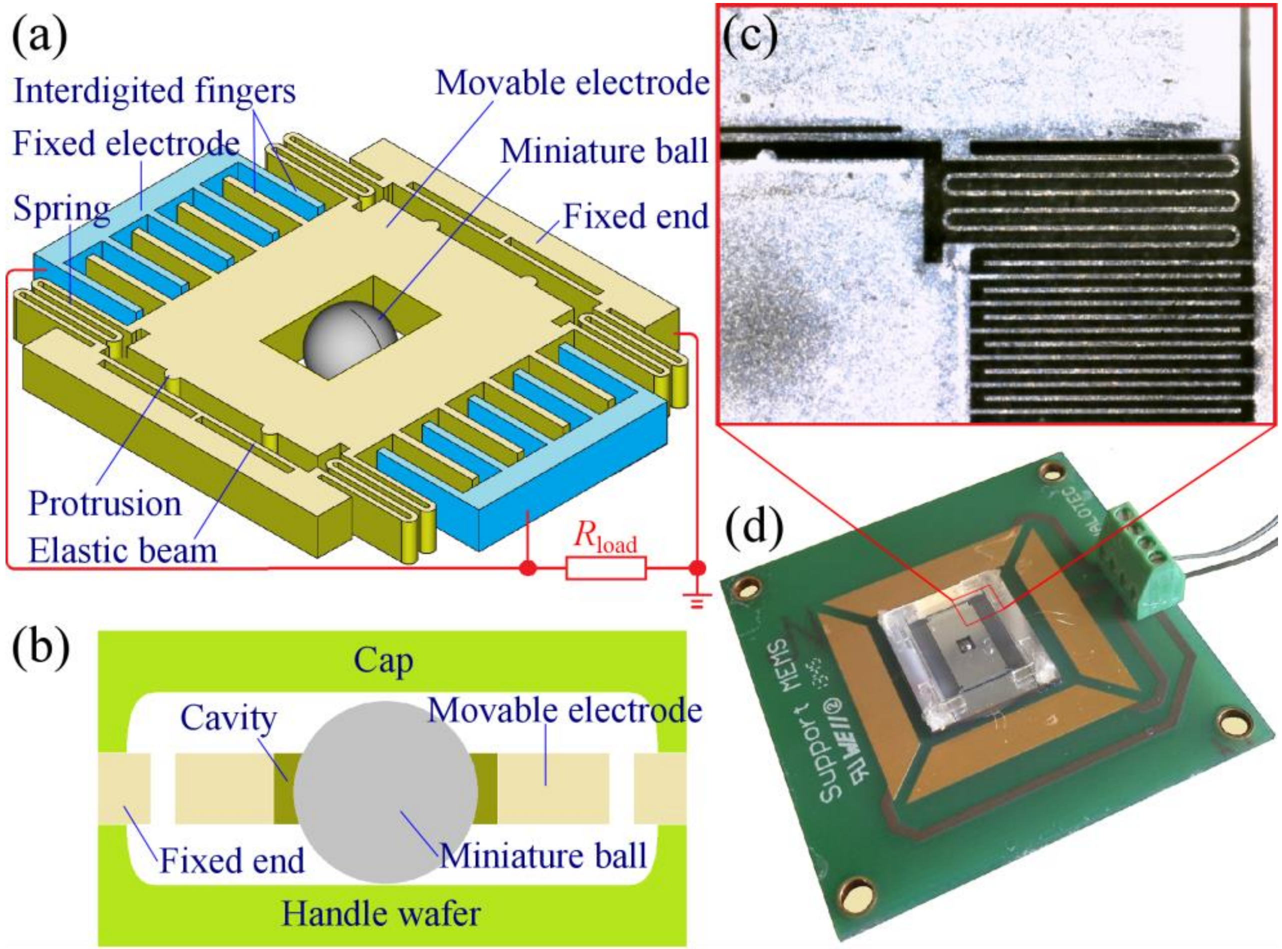

Low-frequency MEMS electrostatic VEH

Experimental test

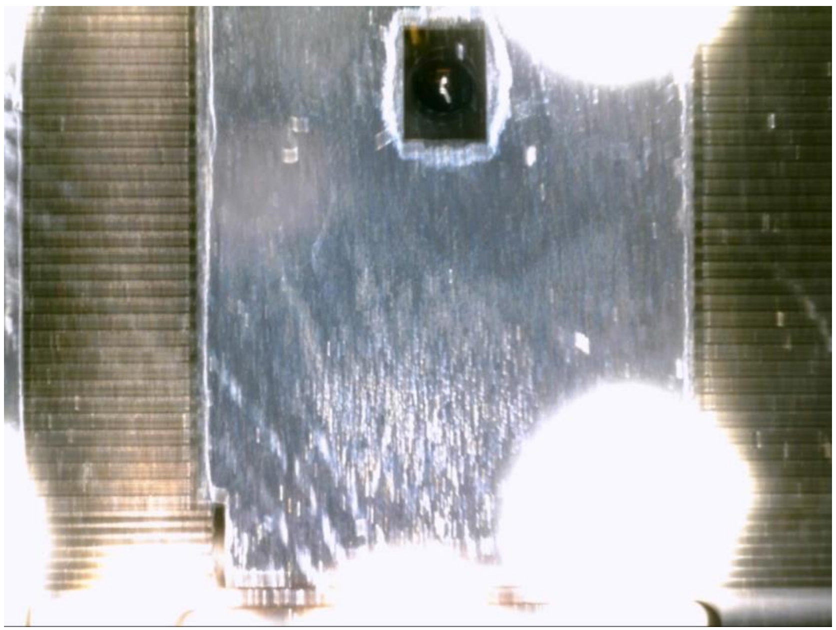

Working principle

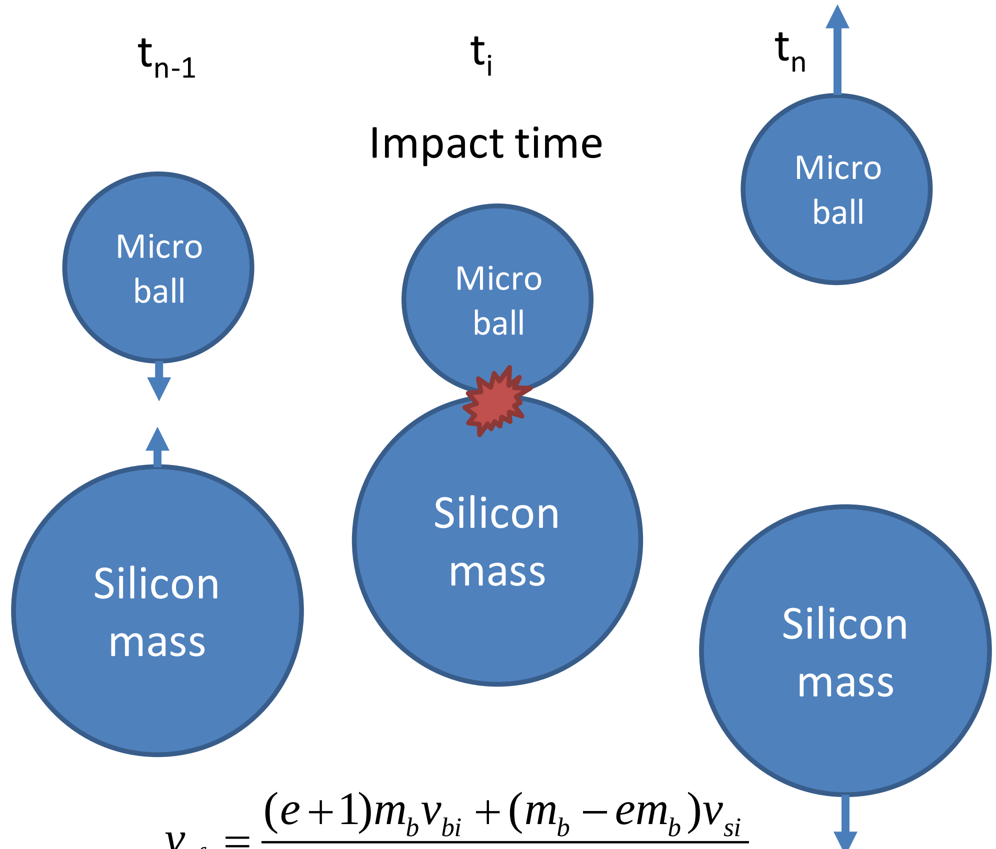

$$v_{sf} = \frac{(e+1)m_b v_{bi} + (m_b - e m_b) v_{si}}{m_b + m_s}$$

Velocity Amplified Energy Harvester
At Stoke Institute, University of Limerick, Ireland

Low-frequency MEMS electrostatic VEH

without micro-ball

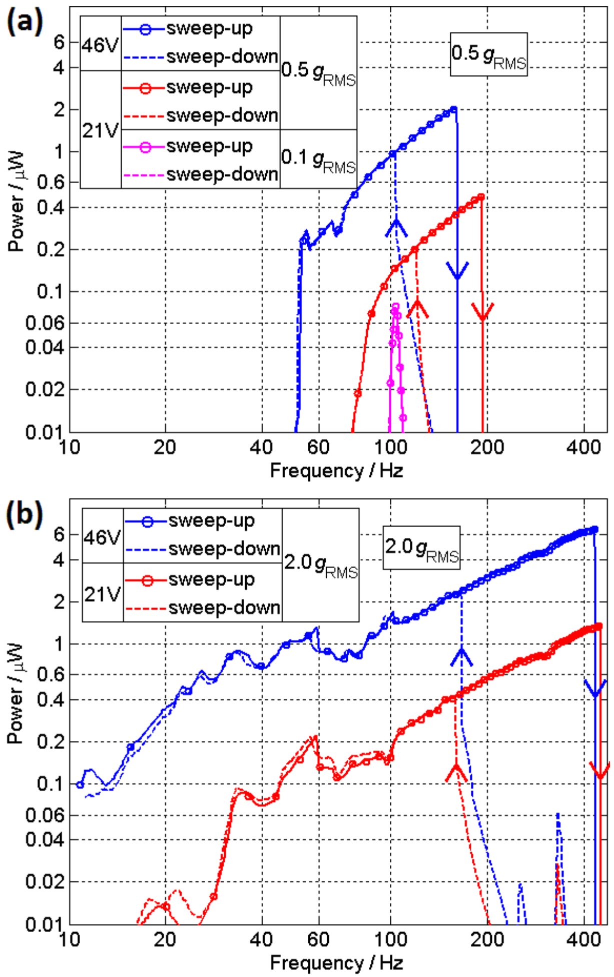

with micro-ball

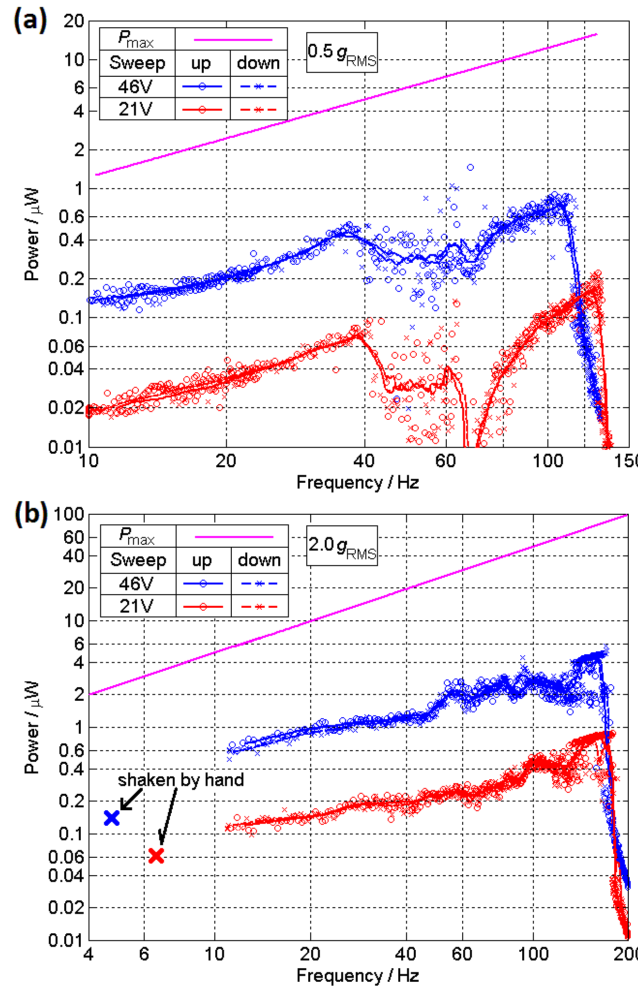

Y. Lu, F. Cottone, S. Boisseau, F. Marty, D. Galayko, and P. Basset, Appl. Phys. Lett. 2015.

Low-frequency MEMS electrostatic VEH

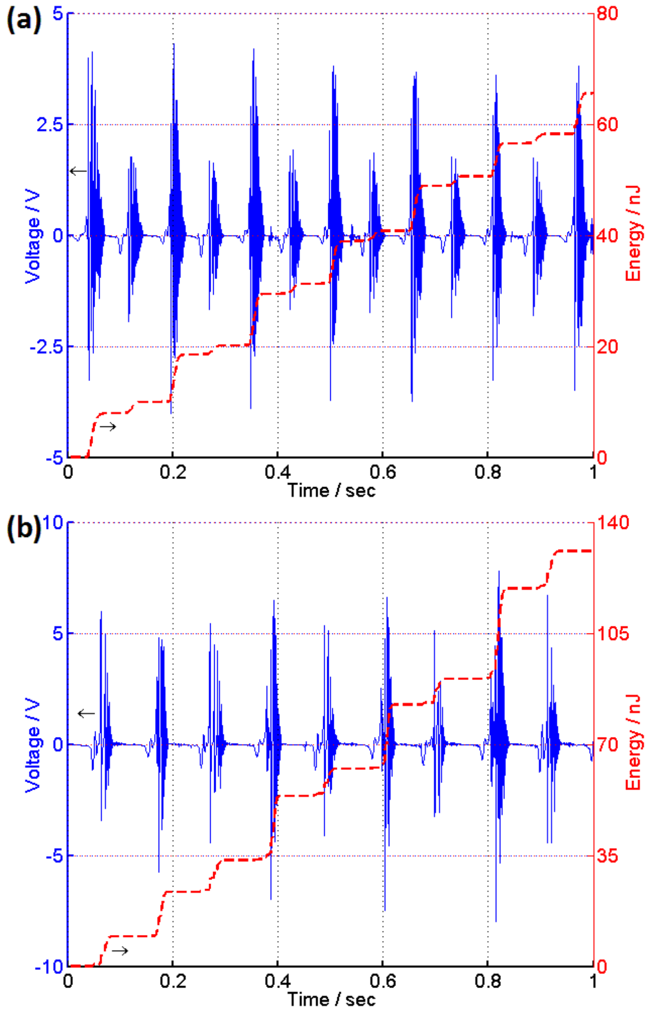

TEST with hand shaking of the transient output voltage and extracted energy.

(a) Vbias=21 V, a=2.0 grms, f=6.5 Hz;
(b) Vbias=46 V, a=2.0 grms, f=4.7 Hz

A 47-µF capacitor has been also charged through a bridge diode rectifier to 3.5 V to supply a wireless temperature sensor node.

Y. Lu, F. Cottone, S. Boisseau, F. Marty, D. Galayko, and P. Basset, Appl. Phys. Lett. 2015.

Performance comparison

Vibration type	MEMS Direction	Accel. (gRMS)	Main input Freq. (Hz)	Vbias (V)	Power (uW)	Power Density (uW/cm3)
Man walking	X	0.39	4.15	20	1.34	13.40
Man walking	Y	0.27	2.1	20	0.793	7.93
Man walking	Z	0.41	2.44	20	1.15	11.50
Man running	Z	1.20	3.3	20	14.9	142.00

Table 2 Comparison of Effectiveness of Published Electrostatic Motion Harvesters

Author	Reference	Generator Volume [cm^3]	Proof Mass [g]	Input Amplitude [μm]	Input Frequency [Hz]	Z_l [μm]	Power (unprocessed) [μW]	Power (processed) [μW]	Power Density [$\mu W/cm^3$]	Harvester Effectiveness [%]	Volume Figure of Merit [%]
Tashiro	[104]		640	380	4.76	19000		58		0.09	
Tashiro	[142]	15	780	9000	6		36		2.42		0.02
Mizuno	[108]	0.6	0.7	0.64	743	4.9	7.4×10^{-6}		1.23×10^{-3}	6.6×10^{-6}	1.86×10^{-9}
Miyazaki	[143]		5	1	45	30		0.21		12.4	
Arakawa	[144]	0.4	0.65	1000	10	1000	6		15	7.42	0.68
Despesse	[145]	18	104	90	50	90	1760	1000	56	7.66	0.06
Yen	[146]				1500			1.8			
Tsutsumino	[147]			600	20	600	278				
Tsutsumino	[148]			1000	20	1000	6.4				
Mitcheson	[109]	0.6	0.12	1130	20	100	2.4		4	17.9	0.02

Almost 1 order of magnitude higher than average power density of previous works

P. D. Mitcheson, et al, *Proceedings of the IEEE,* vol. 96, pp. 1457-1486, 2008.

Final considerations

- **Energy harvesting systems** will enable low-power Technology to be completely autonomous

- **Energy harvesting systems** can be improved by:
  - Nonlinear dynamic: bistable systems, freqeuncy-up converters, impacting masses, electrostatic softening
  - Innovative electro-active materials (electrets, lead-free piezo)
  - Miniaturization: research on innovative nanostructured piezoelectric, magnetic and electrets materials, frequency-up conversion

- There is need for improvement for **low-power electronics**
  - Low-consumption components
  - Efficient conditioning circuit
  - Power-aware software